Supplemental Material (not copyedited or formatted) for: Simran K. Sandhu, Andrew Yu. Morozov, Robert D. Holt, Michael Barfield. 2021. "Revisiting the Role of Hyperparasitism in the Evolution of Virulence." The American Naturalist 197(2). DOI: https://doi.org/10.1086/712351.

Supplementary Material: Revisiting the Role of Hyperparasitism in Evolution of Virulence

Simran K. Sandhu[1]
Andrew Yu. Morozov[1,2,3*]
Robert D. Holt[4]
Michael Barfield[4]

September 17, 2020

1. Department of Mathematics, University of Leicester, LE1 7RH, UK;
2. Institute of Ecology and Evolution, Russian Academy of Sciences, Moscow, Russia
3. Lobachevsky State University of Nizhni Novgorod, Nizhniy Novgorod, Russia
4. Department of Biology, University of Florida, FL 32611, USA;
∗ Corresponding author; e-mail: am379@le.ac.uk.

Contents

SM1 Model Flowcharts

Within Section 2 of the of the main text, we introduce a generic host-parasite-hyperparasite model which allows for the dynamics of multiple strains of parasite and hyperparasite to be considered. This model is described by equations (1)-(3) in the main manuscript. The addition of different strains can result in quite a complex model, hence, we display the dynamics in the form of a flowchart, shown in Fig. S1.

In Section 3 of the main text, we considered three different possible evolutionary scenarios, for each of these scenarios we constructed similar flowcharts depicting the interactions with the resident-mutant models constructed using the adaptive dynamics framework. The first scenario in Section 3.1 considers the evolution in the parasite only, when the parasite virulence can evolve but the hyperparasite strength is fixed. The flowchart for this scenario is shown in Fig. S2.

Supplemental Material (not copyedited or formatted) for: Simran K. Sandhu, Andrew Yu. Morozov, Robert D. Holt, Michael Barfield. 2021. "Revisiting the Role of Hyperparasitism in the Evolution of Virulence." The American Naturalist 197(2). DOI: https://doi.org/10.1086/712351.

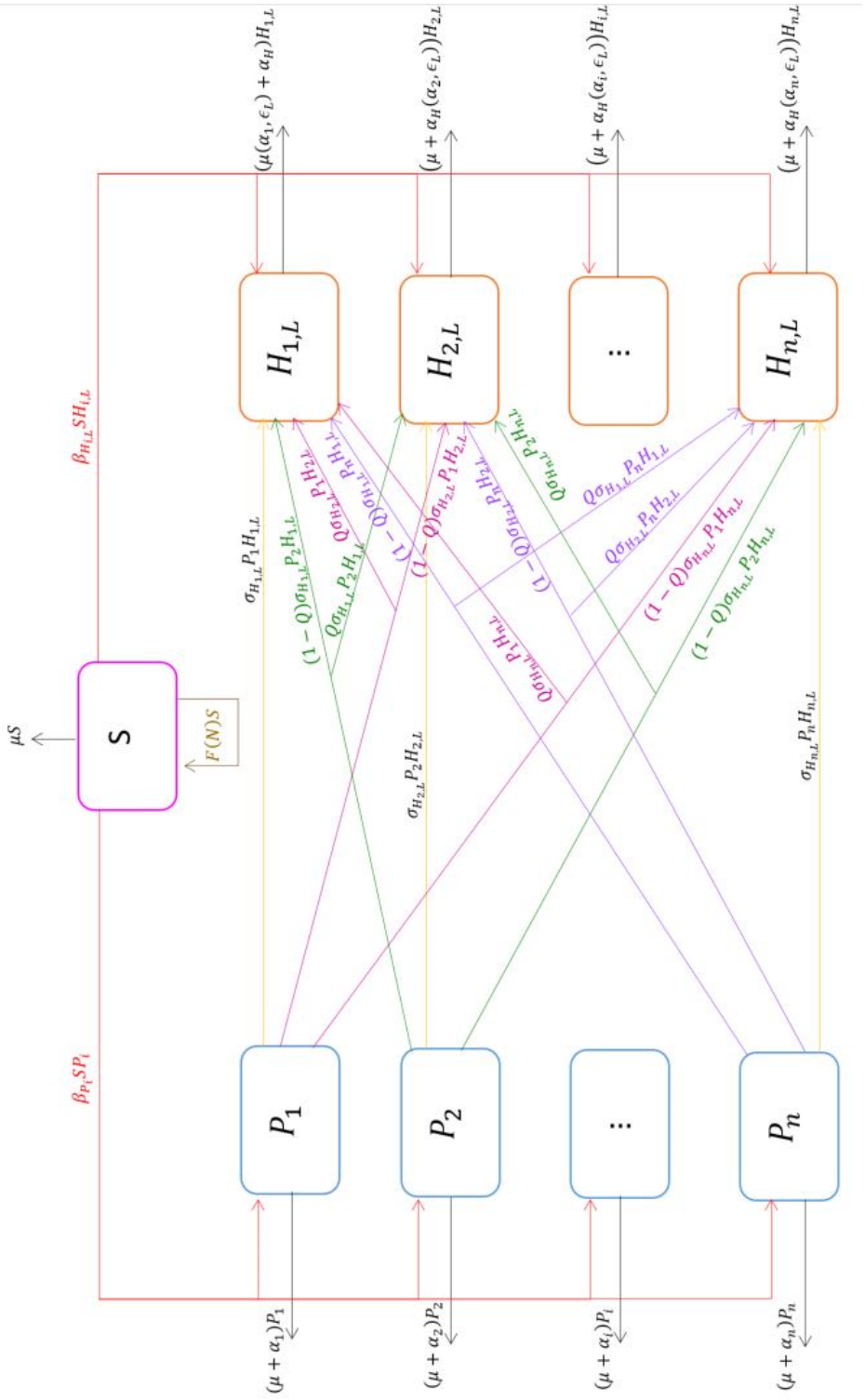

Figure S1: Flowchart displaying all interactions within the generic host-parasite-hyperparasite model that accounts for the existence of multiple strains of parasite and hyperparasite, given in the main text by equations (1)-(3). The system consists of three components; healthy hosts (S), hosts infected by a parasite (P_i) and hosts infected by a hyperparasite ($H_{i,L}$) where i denotes the parasite strain with virulence α_i and L represents the hyperparasite with strength ϵ_L. For the sake of simplicity the figure includes only a single strain of the hyperparasite L.

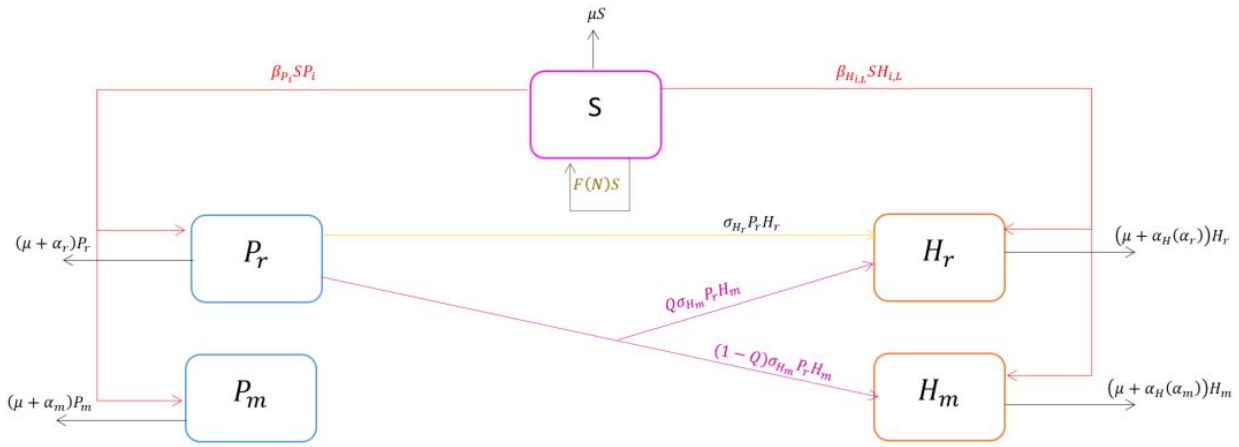

Figure S2: Flowchart for the introduction of an initially rare mutant strain with virulence α_m into the ecological equilibrium of resident strain α_r as described in Section 3.1 of the main text where evolution in the parasite only is considered.

Next, in Section 3.2 we fixed the parasite virulence and considered evolution in the hyperparasite strength only. The corresponding flowchart can be seen in Fig. S3.

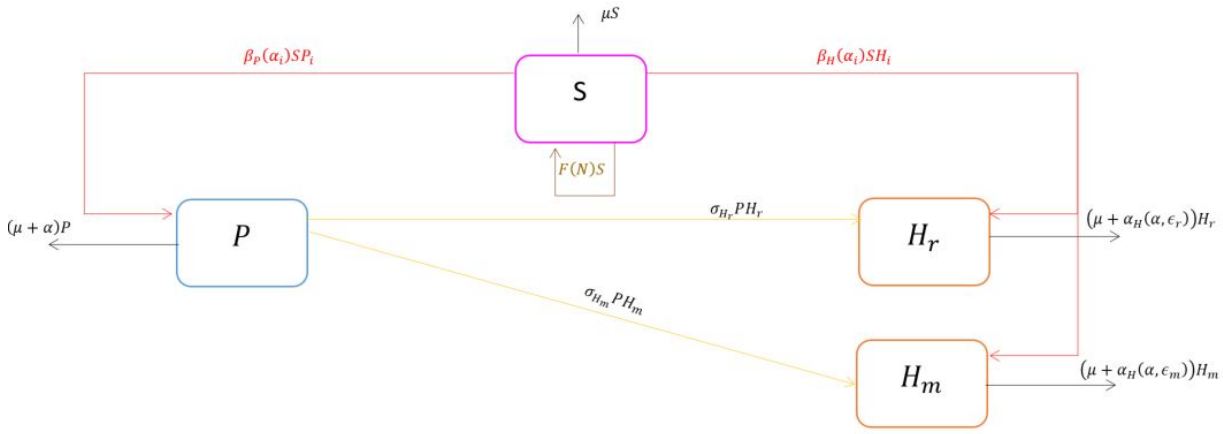

Figure S3: Flowchart for the introduction of a rare mutant hyperparasite strain ϵ_m into the resident system characterised by ϵ_r at its ecological equilibrium, where the parasite virulence α is fixed. This corresponds to the mutant equation (12) given in Section 3.2 of the main text.

Finally, we consider the co-evolution of both the parasite virulence and the hyperparasite strength. This scenario corresponds to Section 3.3 within the main text. The flowchart for this scenario is shown in Fig. S4.

Supplemental Material (not copyedited or formatted) for: Simran K. Sandhu, Andrew Yu. Morozov, Robert D. Holt, Michael Barfield. 2021. "Revisiting the Role of Hyperparasitism in the Evolution of Virulence." The American Naturalist 197(2). DOI: https://doi.org/10.1086/712351.

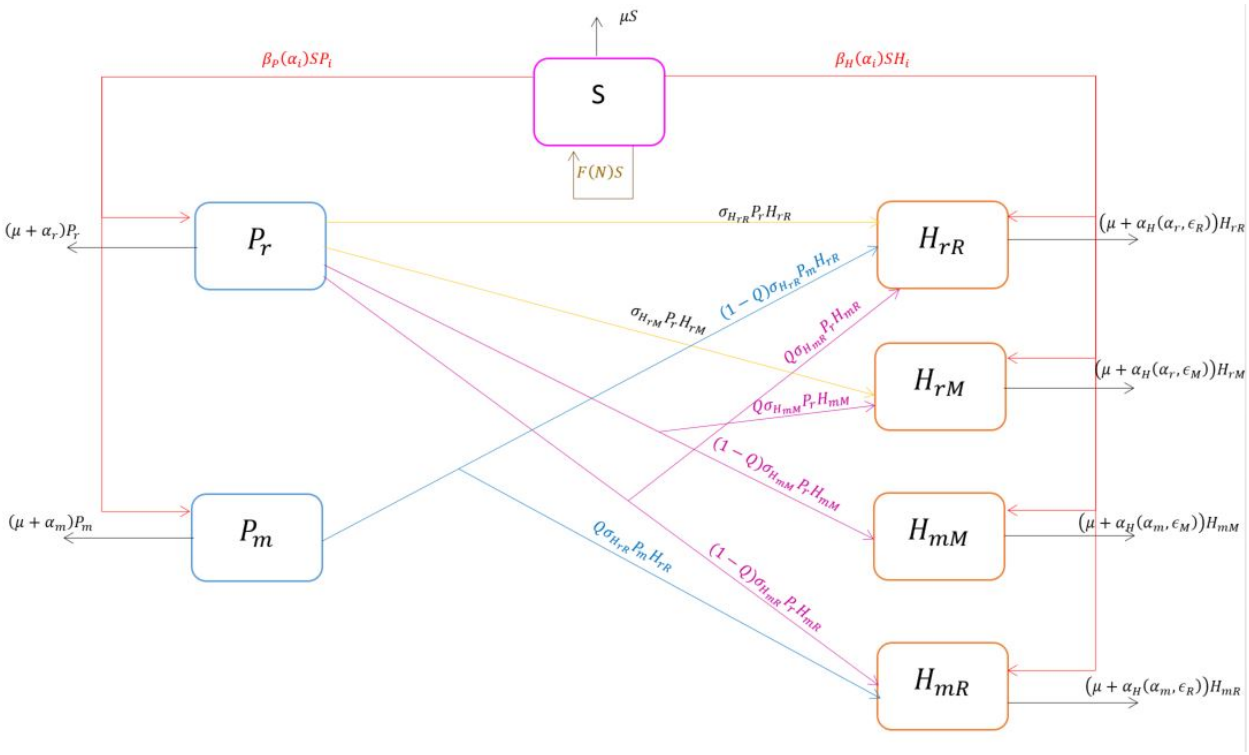

Figure S4: Flowchart for the mutant-resident model corresponding to Section 3.3 of the main text where we allow for the co-evolution of both the parasite virulence and the hyperparasite strength. The resident components S, P_r and $H_{r,R}$ assume parasite virulence α_r and hyperparasite strength ϵ_R. The mutant components allow for a mutation in just the hyperparasite producing $H_{r,M}$, a mutation in just the parasite producing P_m, $H_{m,R}$ and a simultaneous mutation in both producing P_m, $H_{m,M}$.

Supplemental Material (not copyedited or formatted) for: Simran K. Sandhu, Andrew Yu. Morozov, Robert D. Holt, Michael Barfield. 2021. "Revisiting the Role of Hyperparasitism in the Evolution of Virulence." The American Naturalist 197(2). DOI: https://doi.org/10.1086/712351.

SM2 Dependence of Evolutionary Outcomes on Key Model Parameters

Within Section 3 of the main manuscript, we looked at the dependence of evolutionary parameters and model dynamics on key parameters.

SM2.1 Evolution in the Parasite Only

Dependence of Prevalence and Mortality on μ In particular, we looked at how the evolutionary parameters and the stationary states varied as we varied μ. Here we show the corresponding figures for the prevalence and the overall mortality and transmission rates. We define the overall mortality to be the average morality for all organisms, given as $\frac{\mu S+\mu P+\alpha P+\mu H+\alpha_H(\alpha)H}{N}$ whereas the overall transmission rate is defined to be the per capita loss of susceptible hosts due to infection via parasites that are either uninfected or infected by the hyperparasite, given as $\beta_P(\alpha)P^* + \beta_H(\alpha,\epsilon)H^*$. Firstly, we looked at the evolution in the parasite only, discussed in Section 3.1 of the main text. The results for this are shown in Fig. S5-S6.

Supplemental Material (not copyedited or formatted) for: Simran K. Sandhu, Andrew Yu. Morozov, Robert D. Holt, Michael Barfield. 2021. "Revisiting the Role of Hyperparasitism in the Evolution of Virulence." The American Naturalist 197(2). DOI: https://doi.org/10.1086/712351.

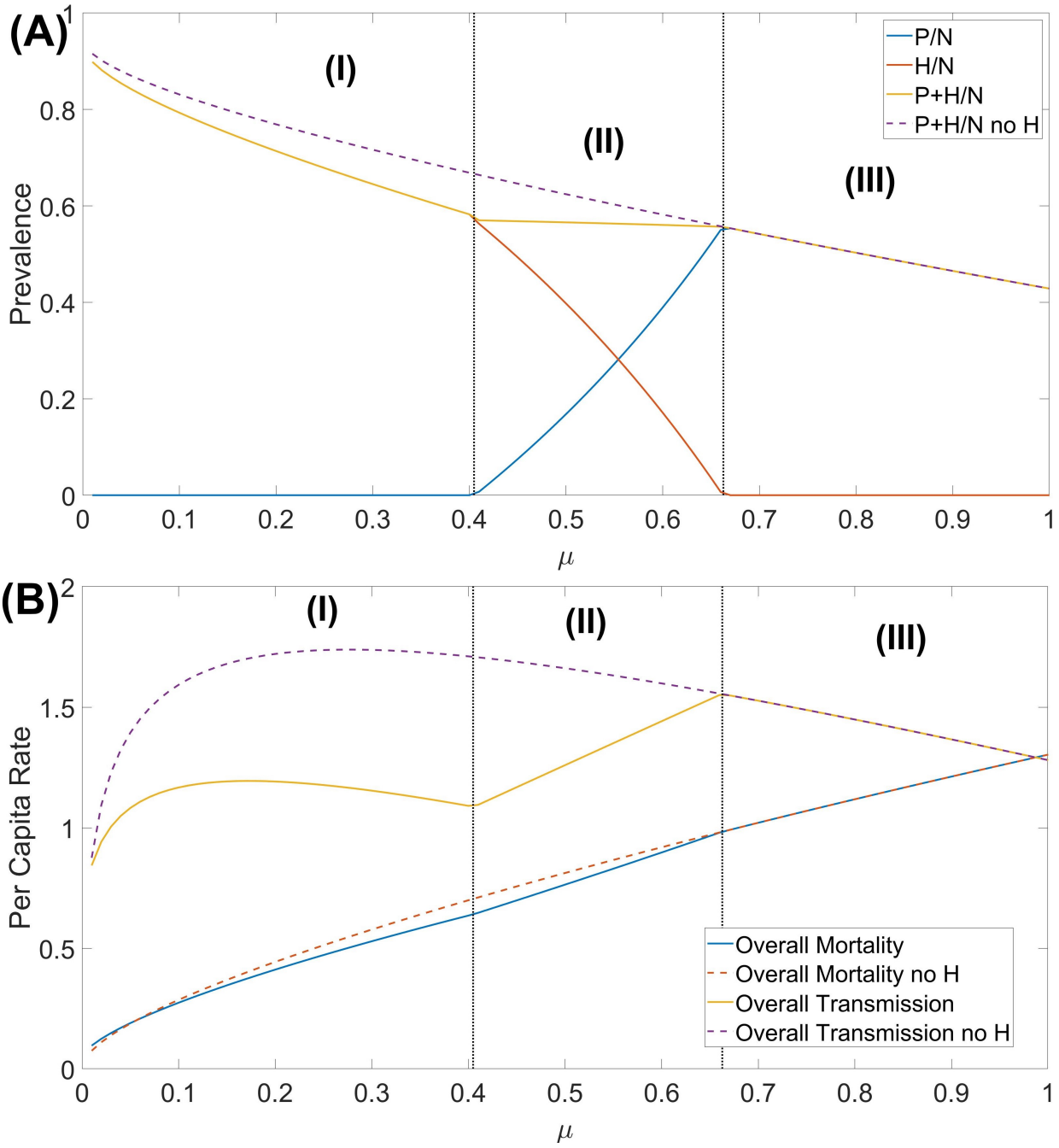

Figure S5: The dependence of model dynamics on the mortality rate μ where we allow for evolution in the parasite only corresponding to Fig. 1 of Section 3.1 of the main text. (A) The dependence on μ of the ESS prevalence of infected hosts in the presence and absence of the hyperparasite. (B) The dependence on μ of the overall mortality and transmission in the presence and absence of the hyperparasite demonstrating the positive impact the introduction of a hyperparasite can have on the host population. Regions (I)-(III) are defined the same as in Fig. 1 of the main manuscript. Other parameter values are as follows: $F(N) = 5 - 0.8N$, $\alpha_0 = 0.6$, $C = 1.5$, $K = 0.5$, $\beta_0 = 0.5$, $Q = 0.9$, $\sigma_0 = 0.5$.

In addition to the example shown in Fig. 1 of the main text and Fig. S5 we also looked at the impact of the background mortality μ when we have a larger fixed value of α_0. We again vary the value of μ and investigate its impact on the ESS, stationary states, prevalence and overall mortality shown in Fig. S6.

Supplemental Material (not copyedited or formatted) for: Simran K. Sandhu, Andrew Yu. Morozov, Robert D. Holt, Michael Barfield. 2021. "Revisiting the Role of Hyperparasitism in the Evolution of Virulence." The American Naturalist 197(2). DOI: https://doi.org/10.1086/712351.

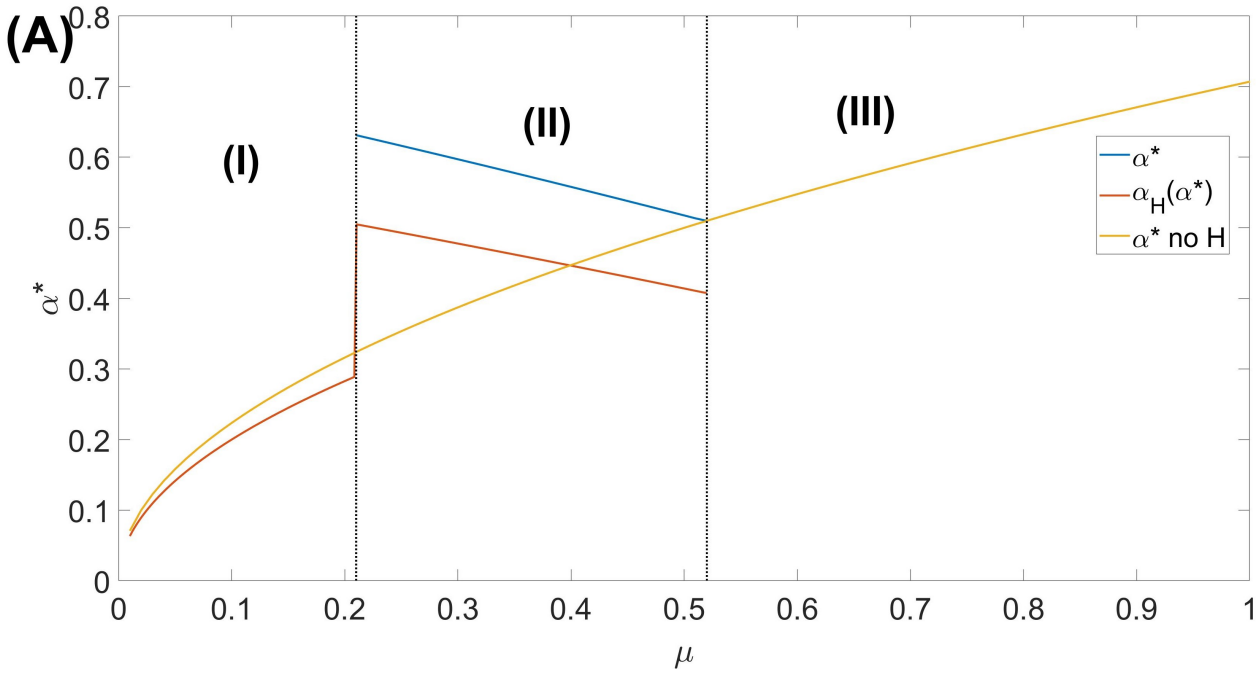

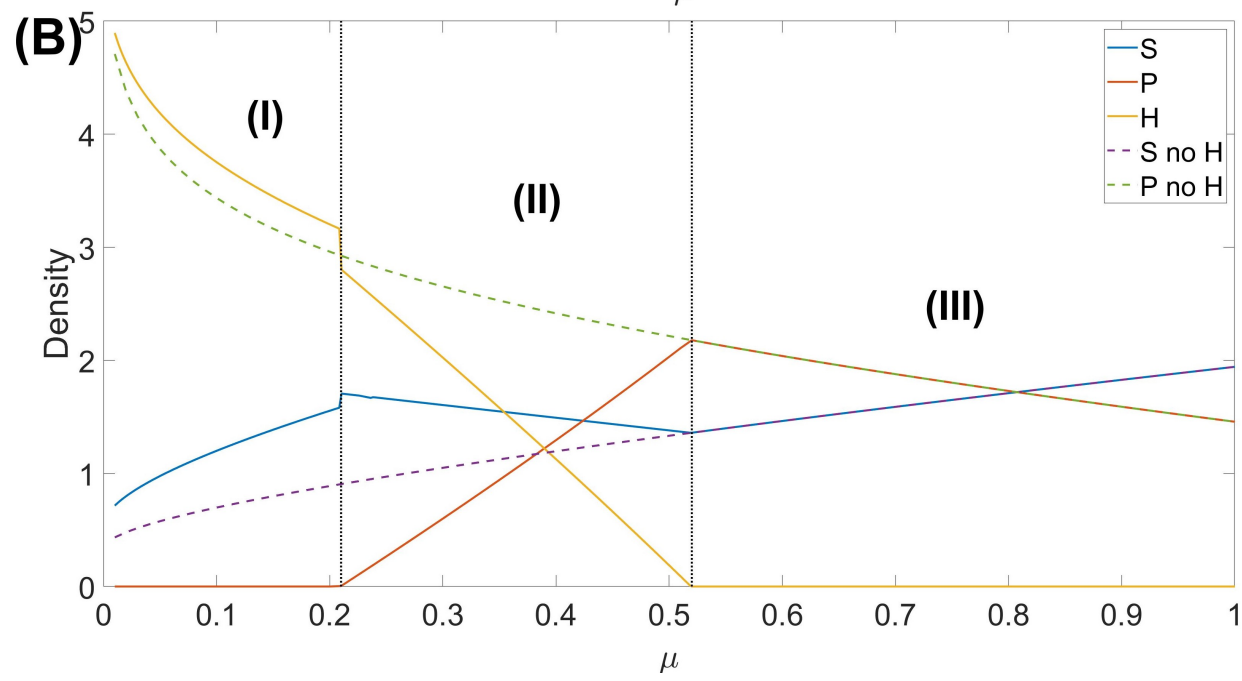

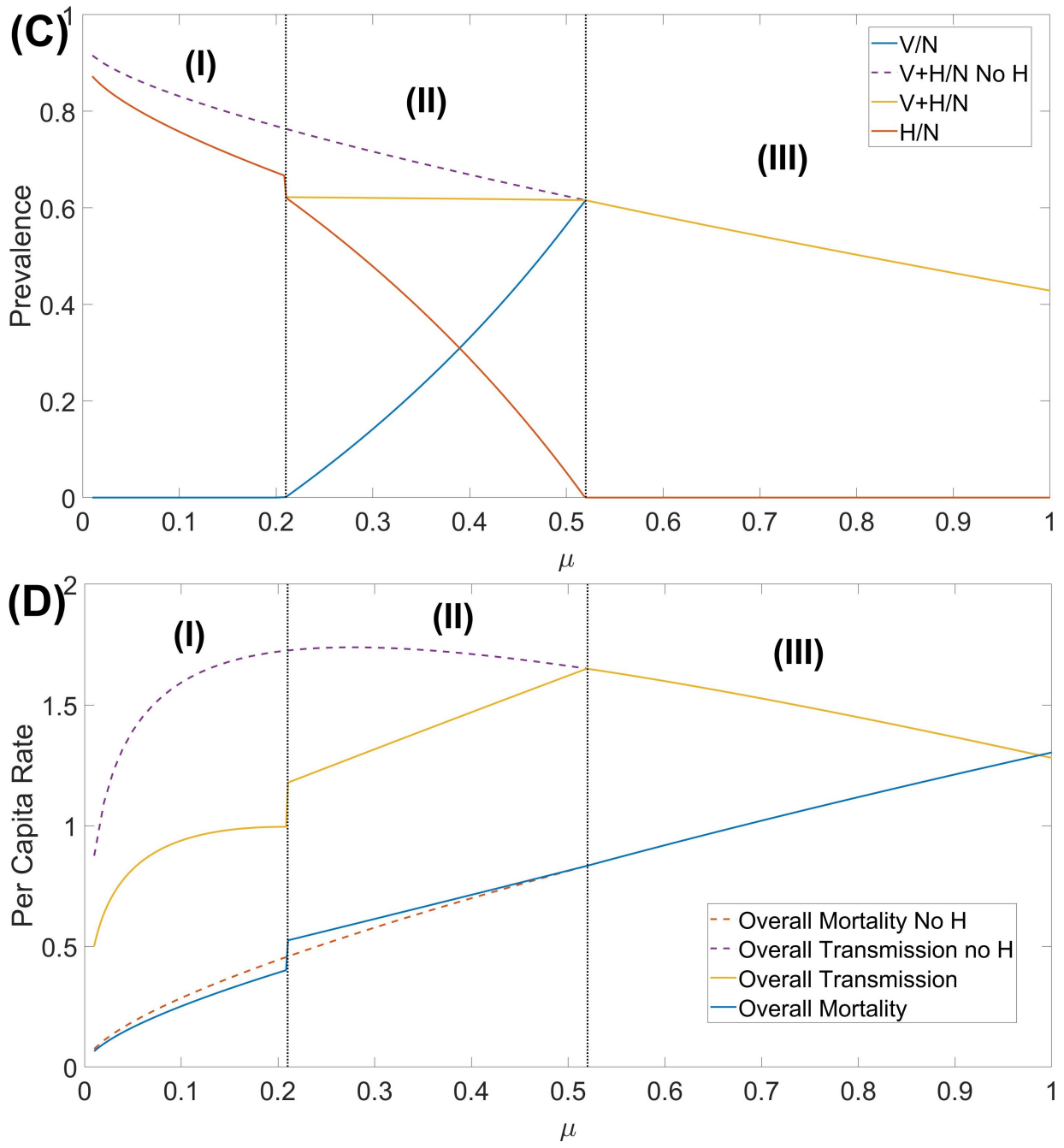

Figure S6: The dependence of model dynamics on the mortality rate μ where we allow for evolution in the parasite only where the hyperparasite has a higher fixed detrimental impact on parasite virulence with $\alpha_0 = 0.8$. (A) The ESS for the case with hyperparasite and without hyperparasite. (B) The equilibrium host densities at the ESS shown in (A). (C) The dependence of the prevalence of both types of infected hosts in the presence and absence of the hyperparasite. (D) The dependence of the overall mortality and transmission in the presence and absence of the hyperparasite demonstrating the positive impact the introduction of a hyperparasite can have on the host population. Regions (I)-(III) are defined the same as in Fig. 1 of the main manuscript. Other parameter values are as follows: $F(N) = 5 - 0.8N$, $\alpha_0 = 0.8$, $C = 1.5$, $K = 0.5$, $\beta_0 = 0.5$, $Q = 0.9$, $\sigma_0 = 0.5$.

Parasite Virulence Dependence on α_0 For the scenario in Section 3.1 where we consider evolution in the parasite only we also investigated the dependence of the model behaviour on the hyperparasite's detrimental effect on the virulence, given by α_0. We vary the value of α_0 (a higher value meaning the hyperparasite lowers pathogen virulence less than for a lower value) and investigate its impact on the ESS, stationary states, prevalence and mortality as shown in Fig. S7.

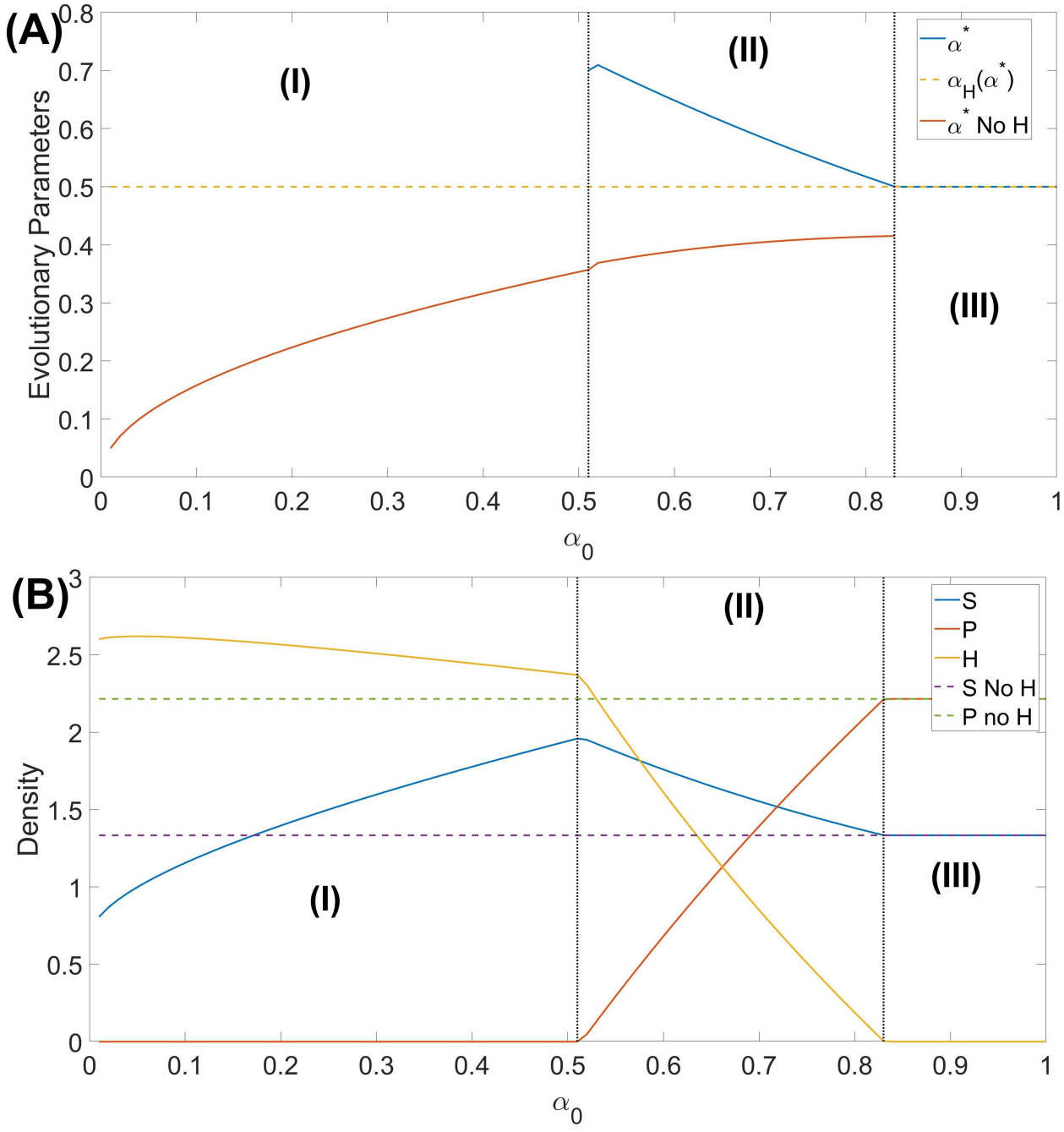

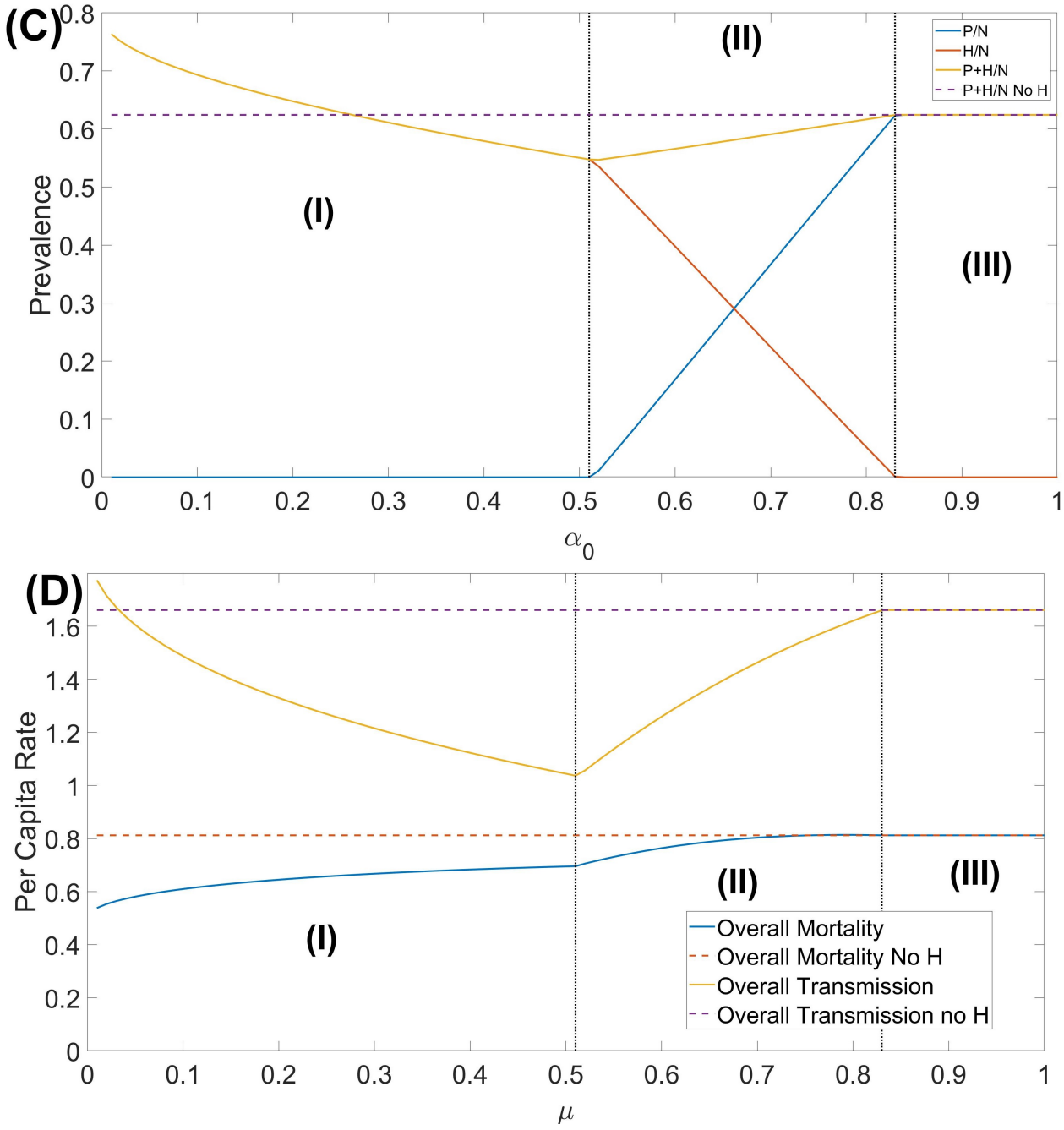

Figure S7: The dependence of model dynamics on the hyperparasite's effect on the parasite virulence, α_0, when we allow for evolution in the parasite only; because this only affects hyperparasites, the "no H" curves do not vary with α_0. (A) The ESS virulence for the case with hyperparasite and without hyperparasite for varying values of α_0. The ratio decreases as α_0 increases, tending towards 1. (B) The stationary states at the ESS shown in (A), there is only coexistence for a small range of α_0 values.(C) The prevalence of the system at the ESS based upon the stationary states in (B). (D) The mortality rates of the system at the ESS based upon the stationary states in (B). Regions (I)-(III) are defined the same as in Fig. 1 of the main manuscript. Other parameter values are as follows: $F(N) = 5 - 0.8N$, $\mu = 0.5$, $C = 1.5$, $K = 0.5$, $\beta_0 = 0.5$, $Q = 0.9$, $\sigma_0 = 0.5$.

From the figure we can see that only for a range of α_0 values can all three types of hosts coexist together;

if α_0 is too small then the parasite becomes hyperparasitised everywhere and if it is too large then the hyperparasite will eventually fall extinct. As α_0 is increased we see that the ESS α^* decreases and tends towards the value of $\widehat{\alpha}$, therefore the more effective or efficient the hyperparasite, the larger the ESS parasite virulence.

One way to assess the effectiveness and benefits of the hyperparasite is to compare the overall mortality rates of all model components for the case with and without hyperparasite. From these mortality rates, it is clear that the addition of an effective hyperparasite (that is, one with a relatively small α_0) results in reduced mortality. Hence the hyperparasite is effective in helping the host to fight against the detrimental effects of the parasite. However, it is interesting to note that for low values of α_0 the healthy host density is lower than and the total transmission can be higher than with no hyperparasites. In these cases the hyperparasite drops parasite virulence much more than transmission, making the parasite more abundant. However, overall mortality is still decreased because of the low virulence.

Parasite Virulence Dependence on β_0 We also investigated the dependence of the ESS parasite virulence α^* and model properties on β_0, the transmission of the hyperparasite-infected parasite β_H relative to that of the uninfected parasite β_P; $0 \leq \beta_0 \leq 1$. As we vary β_0 the changes in the ESS, stationary states, prevalence and mortality rates can be seen in Fig. S8 (note that here we are examining the effect of different fixed values of β_0, and not allowing β_0 to vary as in the hyperparasite evolution and co-evolution scenarios).

Supplemental Material (not copyedited or formatted) for: Simran K. Sandhu, Andrew Yu. Morozov, Robert D. Holt, Michael Barfield. 2021. "Revisiting the Role of Hyperparasitism in the Evolution of Virulence." The American Naturalist 197(2). DOI: https://doi.org/10.1086/712351.

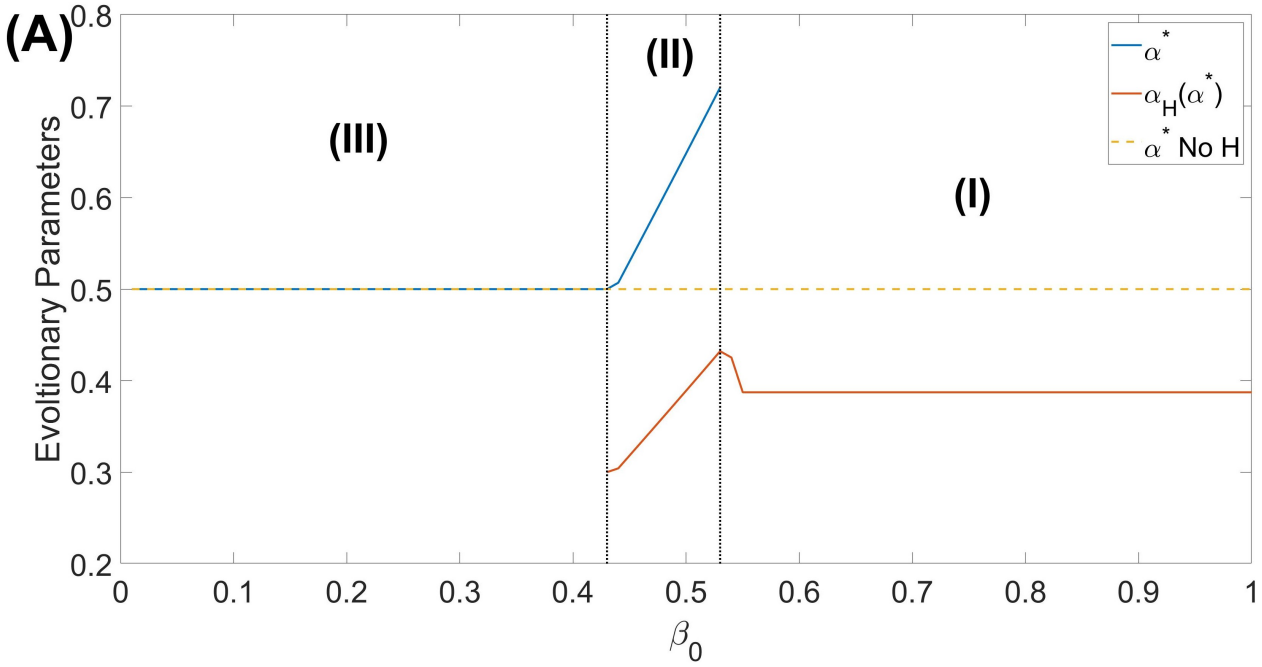

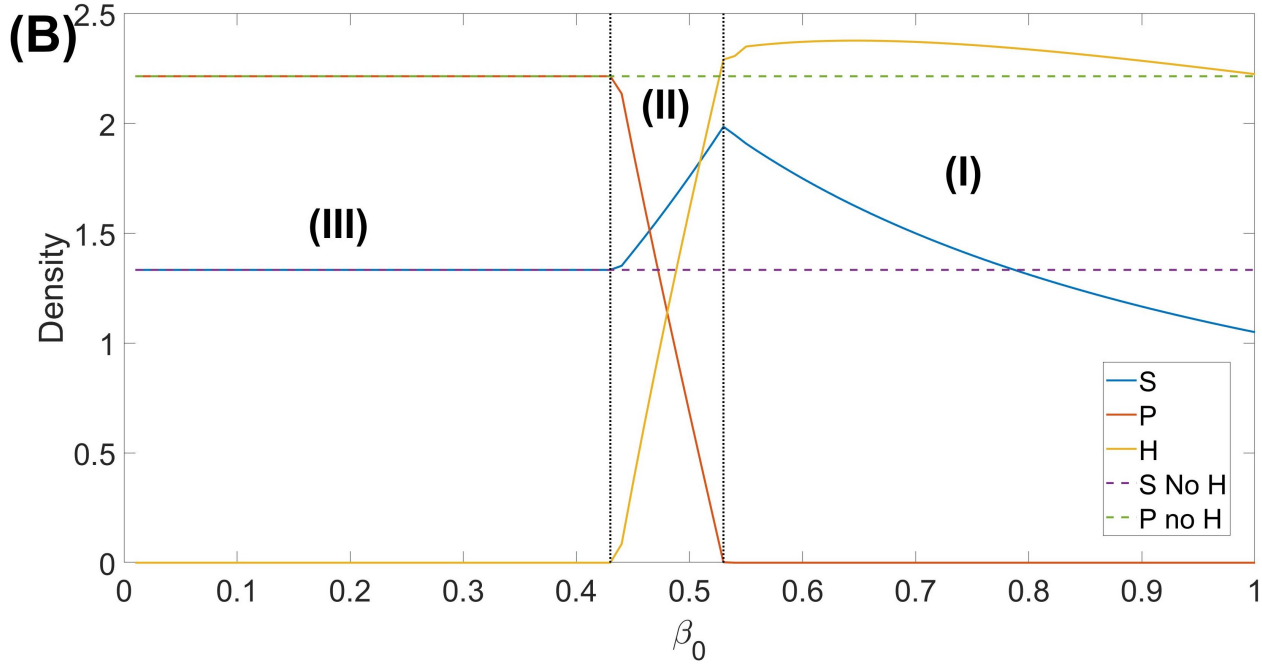

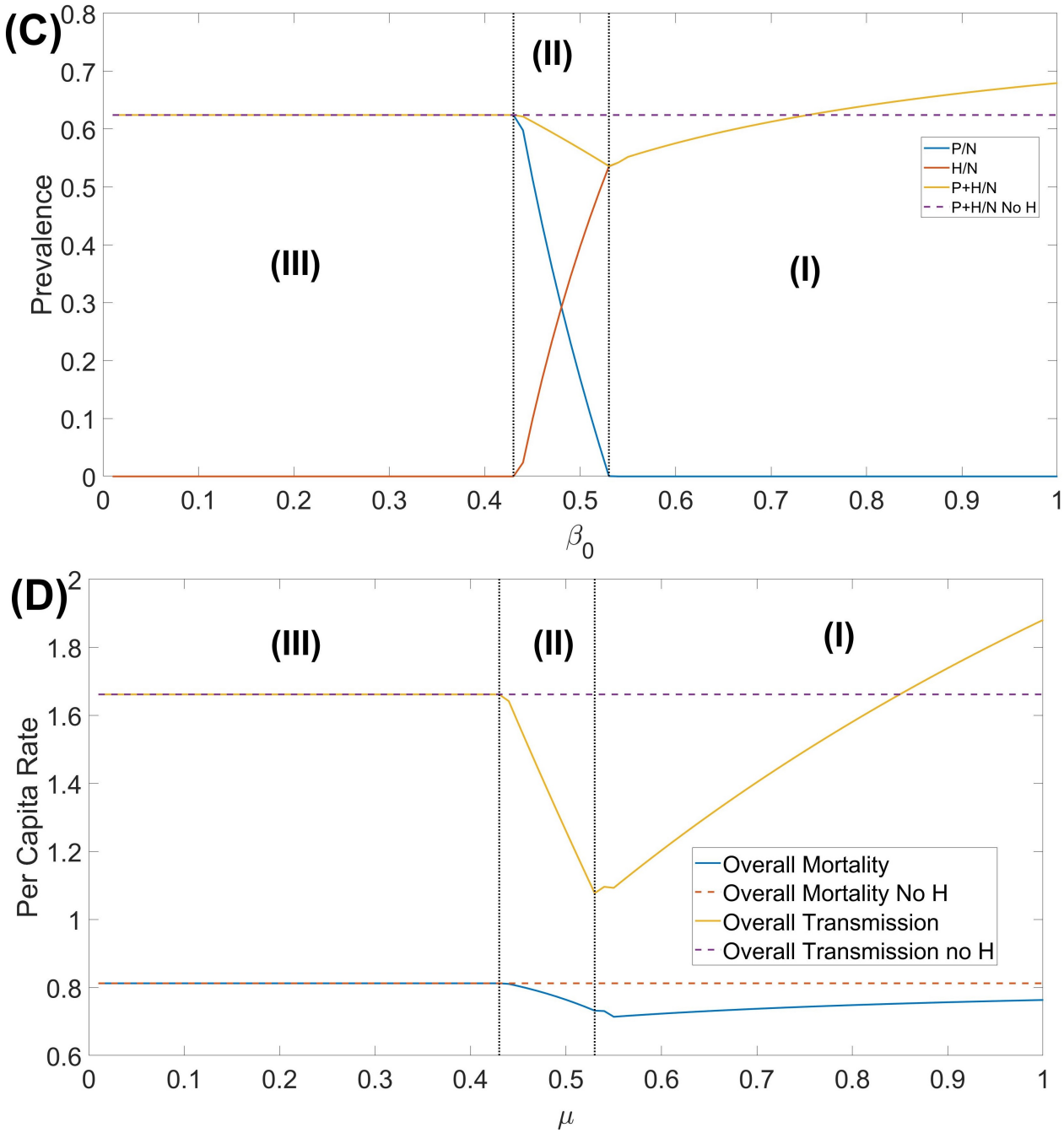

Figure S8: The dependence of model dynamics on the hyperparasite's reduction in the parasite transmission rate, β_0 (a lower value giving a larger reduction), when we allow for evolution in the parasite only. (A) The ESS for the case with hyperparasites and without hyperparasites for varying values of β_0. The ratio decreases as β_0 decreases, tending towards 1. (B) The equilibria at the ESS shown in (A); there is only coexistence for a small range of β_0 values.(C) The prevalence of the system at the ESS based upon the stationary states in (B). (D) The overall mortalities for varying values of β_0. Regions (I)-(III) are defined the same as in Fig. 1 of the main manuscript (but note their reversed positions). Other parameter values are as follows: $F(N) = 5 - 0.8N$, $\mu = 0.5$, $C = 1.5$, $K = 0.5$, $Q = 0.9$, $\sigma_0 = 0.5$, $\alpha_0 = 0.6$.

Again we can assess the effectiveness and benefits of the hyperparasite by comparing the host-parasite-hyperparasite model with the host-parasite model. From this figure, it is clear that the larger the value of

β_0 the greater the impact of the hyperparasite on the system. It can be observed from Fig. S8(D) that the addition of the hyperparasite can potentially reduce the overall mortality provided the hyperparasite has a high enough transmission rate to persist (that is, a large enough value of β_0). Again, it is important to note that for some values of β_0 the healthy host density is less than and the total transmission is greater than the case with no hyperparasite.

SM2.2 Evolution in the Hyperparasite Only

Next, we considered the scenario of evolution in the hyperparasite only, discussed in Section 3.2 of the main text. Fig. 3 shows the dependence of the ESS hyperparasite strength and stationary states on the background mortality μ. In Fig. S9 we show the corresponding figures for the prevalence and overall mortality dependence.

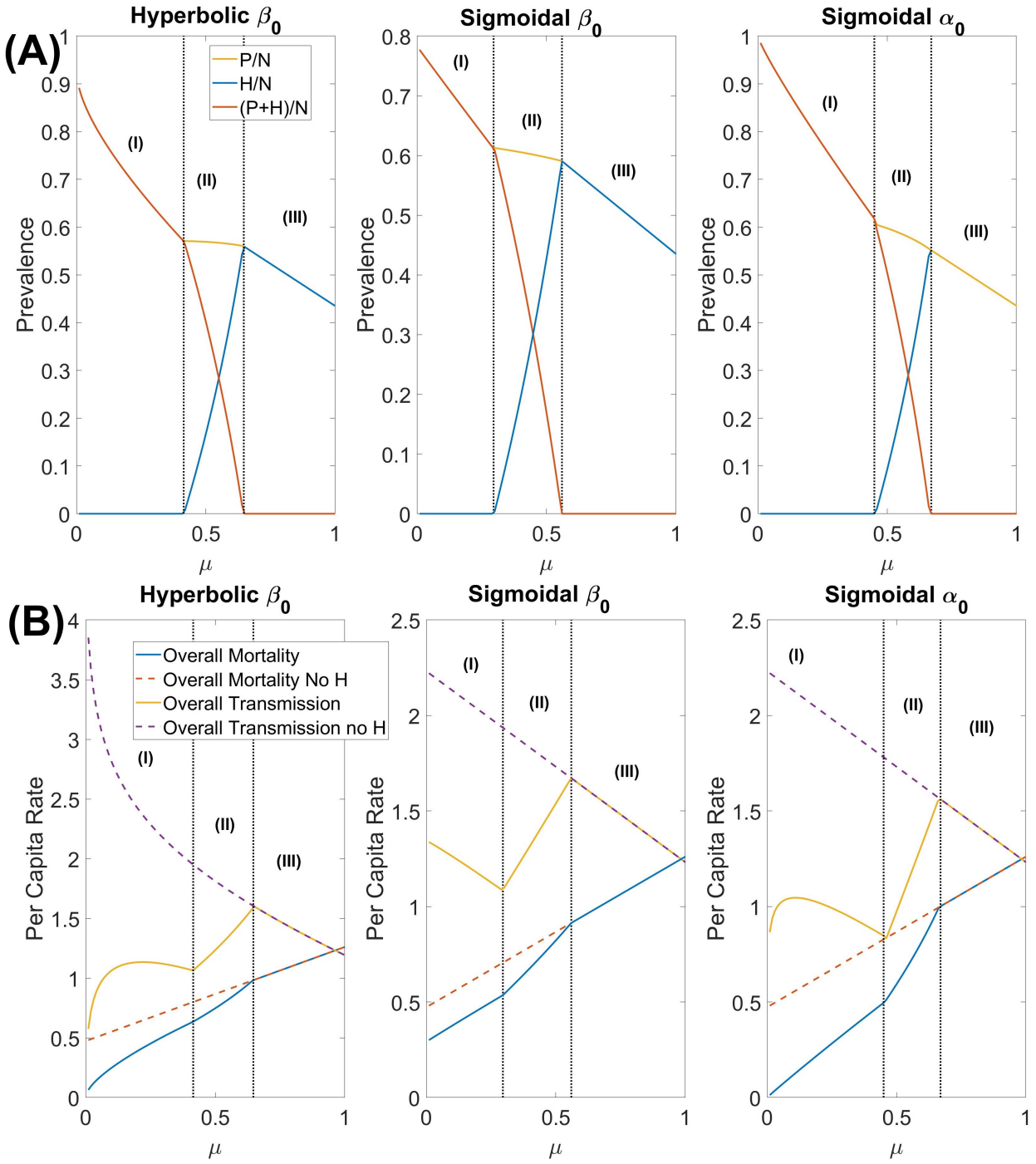

Figure S9: The dependence of model dynamics on the mortality rate μ where we allow for evolution in the hyperparasite only corresponding to Fig. 2 of Section 3.2 of the main text. (A) The dependence of the prevalence of both types of infected hosts. (B) The dependence of the overall mortality and transmission demonstrating the positive impact the introduction of a hyperparasite can have on the host population. Regions (I)-(III) are defined the same as in Fig. 1 of the main manuscript. Other parameter values are as follows; $F(N) = 5 - 0.8N$, $C = 1.5$, $K = 0.5$, $Q = 0.9$, $\sigma_0 = 0.5$ and $\alpha = 0.6$.

Supplemental Material (not copyedited or formatted) for: Simran K. Sandhu, Andrew Yu. Morozov, Robert D. Holt, Michael Barfield. 2021. "Revisiting the Role of Hyperparasitism in the Evolution of Virulence." The American Naturalist 197(2). DOI: https://doi.org/10.1086/712351.

SM2.3 Co-evolution of Parasite and Hyperparasite

Lastly, in Section 3.3 we considered the scenario with co-evolution of both the parasite and hyperparasite. The dependence of the prevalence and overall mortality are shown in Fig. S10 corresponding to Fig. 4 of the main text.

Supplemental Material (not copyedited or formatted) for: Simran K. Sandhu, Andrew Yu. Morozov, Robert D. Holt, Michael Barfield. 2021. "Revisiting the Role of Hyperparasitism in the Evolution of Virulence." The American Naturalist 197(2). DOI: https://doi.org/10.1086/712351.

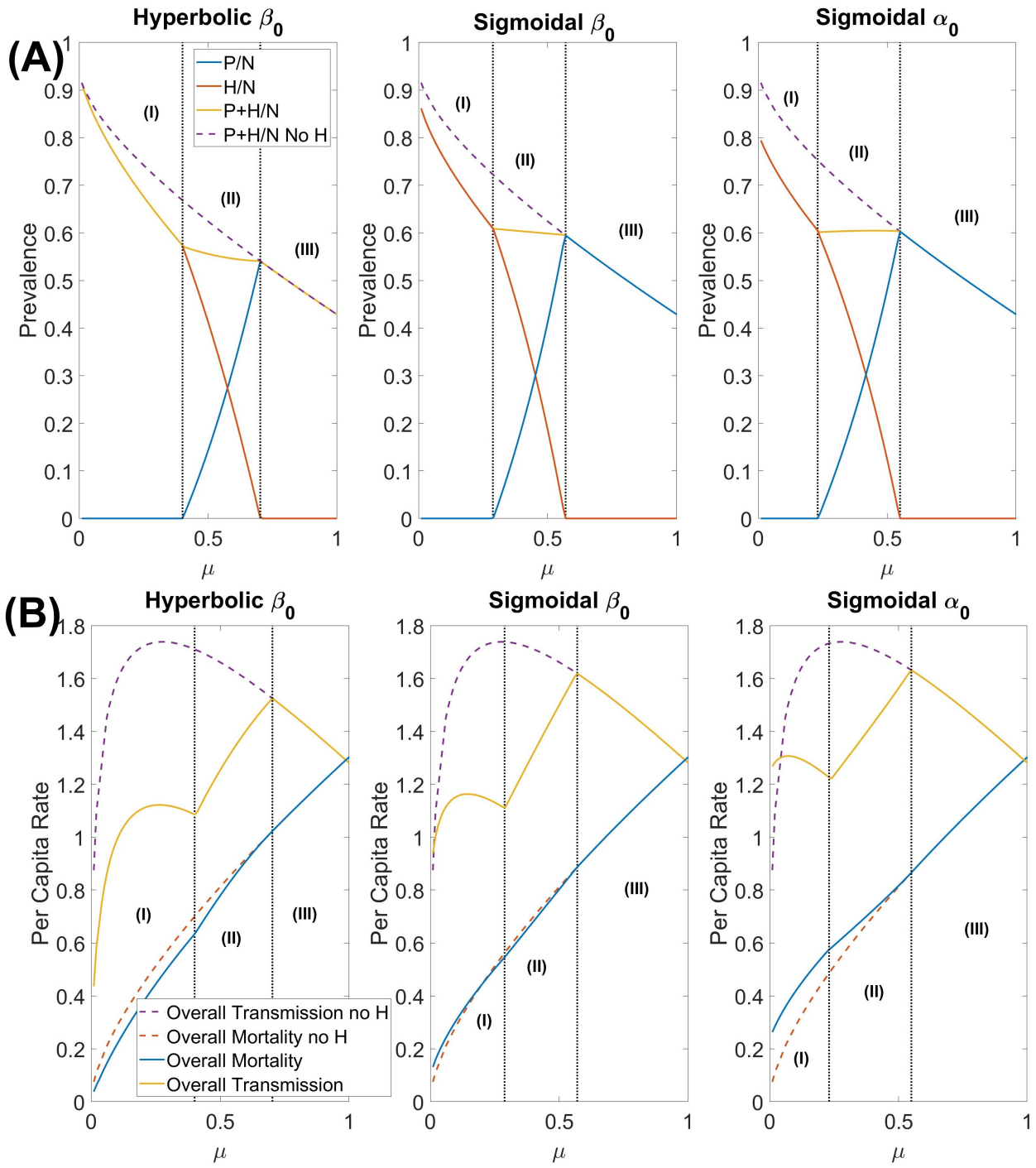

Figure S10: The dependence of model dynamics on the mortality rate μ where we allow for co-evolution in both the parasite and hyperparasite corresponding to Fig. 4 of Section 3.3 of the main text. (A) The dependence of the prevalence of both types of infected hosts in the presence and absence of the hyperparasite. (B) The dependence of the overall mortality in the presence and absence of the hyperparasite demonstrating the positive impact the introduction of a hyperparasite can have on the host population. Regions (I)-(III) are defined the same as in Fig. 1 of the main manuscript. Other parameter values are as follows; $F(N) = 5 - 0.8N$, $C = 1.5$, $K = 0.5$, $Q = 0.9$, $\sigma_0 = 0.5$ and $\alpha = 0.6$.

Supplemental Material (not copyedited or formatted) for: Simran K. Sandhu, Andrew Yu. Morozov, Robert D. Holt, Michael Barfield. 2021. "Revisiting the Role of Hyperparasitism in the Evolution of Virulence." The American Naturalist 197(2). DOI: https://doi.org/10.1086/712351.

SM3 Stability Analysis

This section of the supplementary material provides the analytical stationary states for the trivial, semi-trivial and non-trivial cases for the system with one strain each of parasite and hyperparasite (so we omit subscripts for strain), which are generally defined as the solutions to the following system

$$\frac{dS}{dt} = F(N^*)S^* - \mu S^* - (\beta_P(\alpha)S^*P^* + \beta_H(\alpha)S^*H^*) = 0 \tag{1}$$

$$\frac{dP}{dt} = \beta_P(\alpha)S^*P^* - \sigma(\alpha)P^*H^* - \mu P^* - \alpha P^* = 0 \tag{2}$$

$$\frac{dH}{dt} = \beta_H(\alpha)S^*H^* + \sigma(\alpha)P^*H^* - \mu H^* - \alpha_H(\alpha)H^* = 0 \tag{3}$$

along with their stability conditions determined through the computation of the corresponding Jacobian matrix. When calculating our stationary states we make the following assumptions:

$$F(N) = B_0 - B_1 N$$

$$\alpha_H(\alpha) = \alpha_0 \alpha$$

$$\beta_P(\alpha) = C\frac{\alpha}{\alpha + K} \qquad \beta_H(\alpha) = \beta_0\beta_P(\alpha) \qquad \sigma(\alpha) = \sigma_0\beta_H(\alpha) = \sigma_0\beta_0\beta_P(\alpha).$$

In order to determine the stability of a stationary state we need to determine the eigenvalues of the Jacobian matrix. A stationary state is stable if and only if all eigenvalues $\lambda_{1,2,3}$ have negative real parts.

$(0, 0, 0)$

Initially we consider the trivial case where all organisms are extinct, that is, $(S^*, P^*, H^*) = (0, 0, 0)$. The Jacobian at this stationary state can be simplified to

$$J = \begin{bmatrix} B_0 - \mu & 0 & 0 \\ 0 & -\mu - \alpha & 0 \\ 0 & 0 & -\mu - \alpha_H(\alpha) \end{bmatrix} \tag{4}$$

which has the characteristic equation

$$(B_0 - \mu - \lambda_1)(-\mu - \alpha - \lambda_2)(-\mu - \alpha_H(\alpha) - \lambda_3) = 0 \tag{5}$$

Therefore the eigenvalues are

$$\lambda_1 = B_0 - \mu \tag{6}$$

$$\lambda_2 = -\mu - \alpha \tag{7}$$

$$\lambda_3 = -\mu - \alpha_H(\alpha) \tag{8}$$

$\lambda_2, \lambda_3 < 0$, hence the state is stable when $\lambda_1 < 0$, that is when $B_0 < \mu$. If $B_0 > \mu$ (and hence $\lambda_1 > 0$) then the state $(0, 0, 0)$ is unstable and S will be able to invade this state when initially rare.

$(S_1, 0, 0)$

Now we consider the semi-trivial case for which the parasite is absent, $(S_1, 0, 0)$. We fix $P_1 = 0$ and $H_1 = 0$, and the model at this stationary state is

$$\frac{dS}{dt} = F(S_1)S_1 - \mu S_1 = (B_0 - B_1 S_1)S_1 - \mu S_1 = 0 \tag{9}$$

$$\frac{dP}{dt} = 0 \tag{10}$$

$$\frac{dH}{dt} = 0. \tag{11}$$

The resulting stationary state for the susceptible members is

$$S_1 = \frac{B_0 - \mu}{B_1} \tag{12}$$

The Jacobian at the stationary state $(S_1, 0, 0)$ can be simplified to

$$J = \begin{bmatrix} \mu - B_0 & \mu - B_0 + \beta_P(\alpha)\frac{B_0-\mu}{B_1} & \mu - B_0 - \beta_H(\alpha)\frac{B_0-\mu}{B_1} \\ 0 & \beta_P(\alpha)\frac{B_0-\mu}{B_1} - \mu - \alpha & 0 \\ 0 & 0 & \beta_H(\alpha)\frac{B_0-\mu}{B_1} - \mu - \alpha_H(\alpha) \end{bmatrix} \tag{13}$$

which has the characteristic equation

$$(\mu - B_0 - \lambda_1)(\beta_P(\alpha)\frac{B_0-\mu}{B_1} - \mu - \alpha - \lambda_2)(\beta_H(\alpha)\frac{B_0-\mu}{B_1} - \mu - \alpha_H(\alpha) - \lambda_3) = 0. \tag{14}$$

The eigenvalues are given as

$$\lambda_1 = \mu - B_0 \tag{15}$$

$$\lambda_2 = \beta_P(\alpha)\frac{B_0-\mu}{B_1} - \mu - \alpha \tag{16}$$

$$\lambda_3 = \beta_H(\alpha)\frac{B_0-\mu}{B_1} - \mu - \alpha_H(\alpha) \tag{17}$$

We know $\lambda_1 < 0$ or else $S_1 < 0$ which is not a feasible stationary state. If P is slightly positive rather than 0, its growth can be described as

$$\frac{dP}{dt} = \beta_P(\alpha)\frac{B_0-\mu}{B_1}P - \mu P - \alpha P = \lambda_2 P \tag{18}$$

If the invasion is possible then $\lambda_2 > 0$ and the state $(S_1, 0, 0)$ is unstable. Similarly we have the same condition with λ_3 and the invasion of H. Hence the violation of the stability condition $\lambda_2 < 0$, $\lambda_3 < 0$ results in the possible invasion of P, H respectively.

$(S_2, P_2, 0)$
If we fix $H_2 = 0$, then the model is

$$\frac{dS}{dt} = F(S_2 + P_2)S_2 - \mu S_2 - \beta_P(\alpha)S_2P_2 = 0 \tag{19}$$

$$\frac{dP}{dt} = \beta_P(\alpha)S_2P_2 - \mu P_2 - \alpha P_2 = 0 \tag{20}$$

$$\frac{dH}{dt} = 0. \tag{21}$$

These can be solved to give the following stationary states:

$$S_2 = \frac{\mu + \alpha}{\beta_P(\alpha)} \tag{22}$$

$$P_2 = \frac{B_0 - B_1\frac{\mu+\alpha}{\beta_P(\alpha)} - \mu}{B_1 + \beta_P(\alpha)}. \tag{23}$$

The Jacobian evaluated at this stationary state can be simplified to

$$J = \begin{bmatrix} -B_1S_2 & -(B_1 + \beta_P(\alpha))S_2 & -(B_1 + \beta_H(\alpha))S_2 \\ \beta_P(\alpha)P_2 & 0 & -\sigma(\alpha)P_2 \\ 0 & 0 & \beta_H(\alpha)S_2 + \sigma(\alpha)P_2 - \mu - \alpha_H(\alpha) \end{bmatrix} \tag{24}$$

which has the following characteristic equation:

$$(\beta_H(\alpha)S_2 + \sigma(\alpha)P_2 - \mu - \alpha_H(\alpha) - \lambda_3)(\lambda_{1,2}^2 + B_1\frac{\mu+\alpha}{\beta_P(\alpha)}\lambda_{1,2} + (\mu+\alpha)(B_0 - B_1\frac{\mu+\alpha}{\beta_P(\alpha)} - \mu)) = 0 \tag{25}$$

Provided the real parts of all λ are negative then we have stability, which is true if and only if

$$\lambda_3 = \beta_0(\mu+\alpha) + \frac{\sigma(\alpha)}{B_1+\beta_P(\alpha)}(B_0 - B_1\frac{\mu+\alpha}{\beta_P(\alpha)} - \mu) - \mu - \alpha_H(\alpha) < 0 \tag{26}$$

and

$$B_0 - B_1\frac{\mu+\alpha}{\beta_P(\alpha)} - \mu > 0. \tag{27}$$

Equation (27) is the condition for the real parts of $\lambda_{1,2}$ to be negative. We know $B_0 - B_1\frac{\mu+\alpha}{\beta_P(\alpha)} - \mu > 0$ as if this is not satisfied then $P_2 \leq 0$ which is not feasible. Hence the stability condition is that $\lambda_3 < 0$. As in the previous case $\lambda_3 > 0$ is also the condition for H to successfully invade the state.

$(S_3, 0, H_3)$

Suppose instead the hyperparasite is able to infect the entire parasite population resulting in $P_3 = 0$. Therefore the model is

$$\frac{dS}{dt} = F(S_3+H_3)S_3 - \mu S_3 - \beta_H(\alpha)S_3H_3 = 0 \tag{28}$$

$$\frac{dP}{dt} = 0 \tag{29}$$

$$\frac{dH}{dt} = \beta_H(\alpha)S_3H_3 - \mu H_3 - \alpha_H(\alpha)H_3 = 0. \tag{30}$$

Solving this gives the stationary states

$$S_3 = \frac{\mu+\alpha_H(\alpha)}{\beta_H(\alpha)} \tag{31}$$

$$H_3 = \frac{B_0 - B_1\frac{\mu+\alpha_H(\alpha)}{\beta_H(\alpha)} - \mu}{B_1+\beta_H(\alpha)}. \tag{32}$$

For this scenario the Jacobian is simplified to

$$J = \begin{bmatrix} -B_1S_3 & -(B_1+\beta_P(\alpha))S_3 & -(B_1-\beta_H(\alpha))S_3 \\ 0 & \beta_P(\alpha)S_3 - \sigma(\alpha)H_3 - \mu - \alpha & 0 \\ \beta_H(\alpha)H_3 & \sigma(\alpha)H_3 & 0 \end{bmatrix} \tag{33}$$

which has the following characteristic equation

$$(\beta_P(\alpha)S_3 - \sigma(\alpha)H_3 - \mu - \alpha - \lambda_2)(\lambda_{1,3}^2 + B_1\frac{\mu+\alpha_H(\alpha)}{\beta_H(\alpha)}\lambda_{1,3} + (\mu+\alpha_H(\alpha))(B_0 - B_1\frac{\mu+\alpha_H(\alpha)}{\beta_H(\alpha)} - \mu)) = 0. \tag{34}$$

Provided the real parts of all λ are negative then we have stability, which is true if and only if

$$\lambda_2 = \beta_P(\alpha)\frac{\mu+\alpha_H(\alpha)}{\beta_H(\alpha)} - \frac{\sigma(\alpha)}{B_1+\beta_H(\alpha)}(B_0 - B_1\frac{\mu+\alpha_H(\alpha)}{\beta_H(\alpha)} - \mu) - \mu - \alpha < 0 \tag{35}$$

and

$$B_0 - B_1\frac{\mu+\alpha_H(\alpha)}{\beta_H(\alpha)} - \mu > 0 \tag{36}$$

Again for the state to be feasible ($H_3 > 0$) it is required that $B_0 - B_1\frac{\mu+\alpha_H(\alpha)}{\beta_H(\alpha)} - \mu > 0$. Therefore the stability condition is given by $\lambda_2 < 0$; if this is positive we have the condition for P to increase when rare.

Supplemental Material (not copyedited or formatted) for: Simran K. Sandhu, Andrew Yu. Morozov, Robert D. Holt, Michael Barfield. 2021. "Revisiting the Role of Hyperparasitism in the Evolution of Virulence." The American Naturalist 197(2). DOI: https://doi.org/10.1086/712351.

(S^*, P^*, H^*)

Finally we consider the most complex non-trivial scenario where all model components are able to coexist together. The model is given by equations (1)-(3). The stationary states are

$$S^* = \frac{\alpha\left(\frac{B_1(1-\alpha_0)}{C} - \alpha_0 + \beta_0\right) + \sigma_0\beta_0 B_0 + \frac{B_1(1-\alpha_0)K}{C} - \mu(1-\beta_0+\beta_0\sigma_0)}{B_1(1-\beta_0+\beta_0\sigma_0)} \tag{37}$$

$$P^* = \frac{\mu + \alpha_0\alpha - \beta_0\beta_P(\alpha)S^*}{\sigma_0\beta_0\beta_P(\alpha)} \tag{38}$$

$$H^* = \frac{\beta_P(\alpha)S^* - \mu - \alpha}{\sigma_0\beta_0\beta_P(\alpha)}. \tag{39}$$

Using these stationary states, the Jacobian can be simplified to

$$J = \begin{bmatrix} -B_1S^* & -S^*(B_1+\beta_P(\alpha)) & -S^*(B_1+\beta_0\beta_P(\alpha)) \\ \frac{\mu+\alpha_0\alpha-\beta_0\beta_PS^*}{\sigma_0\beta_0} & 0 & \beta_0\beta_PS^* - \mu - \alpha_0\alpha \\ \frac{\beta_PS^*-\mu-\alpha}{\sigma_0} & \beta_PS^* - \mu - \alpha & 0 \end{bmatrix} \tag{40}$$

The corresponding characteristic equation is given as

$$\begin{aligned} &\sigma_0\beta_0\lambda^3 + \sigma_0\beta_0B_1S^*\lambda^2 - \lambda\left((\beta_H(\alpha)S^* - \mu - \alpha_H(\alpha))(\sigma_0\beta_0(\beta_PS^* - \mu - \alpha) + S^*(B_1+\beta_P(\alpha)))\right) \\ &-\lambda S^*\beta_0(B_1+\beta_H(\alpha))(\beta_PS^* - \mu - \alpha) - (\beta_PS^* - \mu - \alpha)(\beta_H(\alpha)S^* - \mu - \alpha_H(\alpha))\left(S^*B_1(1-\beta_0+\sigma_0\beta_0)\right) = 0 \\ &= a_3\lambda^3 + a_2\lambda^2 + a_1\lambda + a_0 \end{aligned} \tag{41}$$

For a cubic characteristic equation with $a_3 > 0$ (here $a_3 = \sigma_0\beta_0 > 0$), the conditions for stability are $a_2 > 0$, $a_0 > 0$ and $a_2a_1 > a_0$ (Routh-Hurwitz stability condition). The first condition is always satisfied, and the second is assuming that $\beta_0(1-\sigma_0) < 1$, which is true if the hyperparasite decreases transmission as we assume. Therefore, stability is determined by the last condition, which is that

$$\left\{B_1\left(\frac{\beta_P}{\mu+\alpha} - \frac{\beta_H}{\mu+\alpha_H}\right) - \frac{\beta_P}{\mu+\alpha}\frac{\beta_H}{\mu+\alpha_H}(\alpha-\alpha_H)\right\}S^* + \beta_P - \beta_H > 0. \tag{42}$$

The term in braces must be negative for instability assuming that the hyperparasite lowers transmission. The first term in braces must be positive for the equilibrium to be feasible, and the second term is negative assuming that the hyperparasite lowers the death rate.

Since the first term must be positive

$$\begin{aligned} \left\{B_1\left(\frac{\beta_P}{\mu+\alpha} - \frac{\beta_H}{\mu+\alpha_H}\right) - \frac{\beta_P}{\mu+\alpha}\frac{\beta_H}{\mu+\alpha_H}(\alpha-\alpha_H)\right\}S^* + \beta_P - \beta_H > \\ -\frac{\beta_P}{\mu+\alpha}\frac{\beta_H}{\mu+\alpha_H}(\alpha-\alpha_H)S^* + \beta_P - \beta_H. \end{aligned} \tag{43}$$

The first term on the right is negative, and will be most negative if S^* is maximum (assuming the other parameters are not changed; S^* can be increased without changing these parameters), which is when $S^* = \frac{\mu+\alpha_H(\alpha)}{\beta_H}$ (if it is higher, the equilibrium is not feasible, since $P^* < 0$). Therefore

$$-\frac{\beta_P}{\mu+\alpha}\frac{\beta_H}{\mu+\alpha_H}(\alpha-\alpha_H)S^* + \beta_P - \beta_H > (\mu+\alpha_H)\left(\frac{\beta_P}{\mu+\alpha} - \frac{\beta_H}{\mu+\alpha_H}\right). \tag{44}$$

Combining inequalities (43) and (44) gives

$$\left\{B_1\left(\frac{\beta_P}{\mu+\alpha} - \frac{\beta_H}{\mu+\alpha_H}\right) - \frac{\beta_P}{\mu+\alpha}\frac{\beta_H}{\mu+\alpha_H}(\alpha-\alpha_H)\right\}S^* + \beta_P - \beta_H > (\mu+\alpha_H)\left(\frac{\beta_P}{\mu+\alpha} - \frac{\beta_H}{\mu+\alpha_H}\right) \tag{45}$$

But the right hand side is positive under our assumptions, and therefore the left side is positive and the system is stable.

Supplemental Material (not copyedited or formatted) for: Simran K. Sandhu, Andrew Yu. Morozov, Robert D. Holt, Michael Barfield. 2021. "Revisiting the Role of Hyperparasitism in the Evolution of Virulence." The American Naturalist 197(2). DOI: https://doi.org/10.1086/712351.

SM4 Example of Evolutionary Bistability

Within Section 1 of the main text, it is mentioned that we sometimes find evolutionary bistability for our host-parasite-hyperparasite system. Here we provide an example that demonstrates the presence of multiple ESS points. Initially, we suppose that $\alpha = 0.6$ was fixed, that is, we allow evolution in the hyperparasite only. For this we constructed a PIP (shown in Fig.S12(A)) clearly demonstrating two evolutionary attractors. The two attractors are separated by a region for which the hyperparasite is extinct. Following this, we considered the co-evolution of both the parasite and the hyperparasite using the method of quantitative genetics. We consider the trade-off with $\alpha_0 = \frac{0.7}{1+\exp(9-20\epsilon)} + \frac{0.7}{1+\exp(20-25\epsilon)}$ being the sum of two sigmoidal functions and linear $\beta_0 = 0.8\epsilon$, shown in Fig. S11. Note that α_0 can take values greater than one, in which case the hyperparasite increases parasite virulence. However, at both ESSs the hyperparasite reduces virulence.

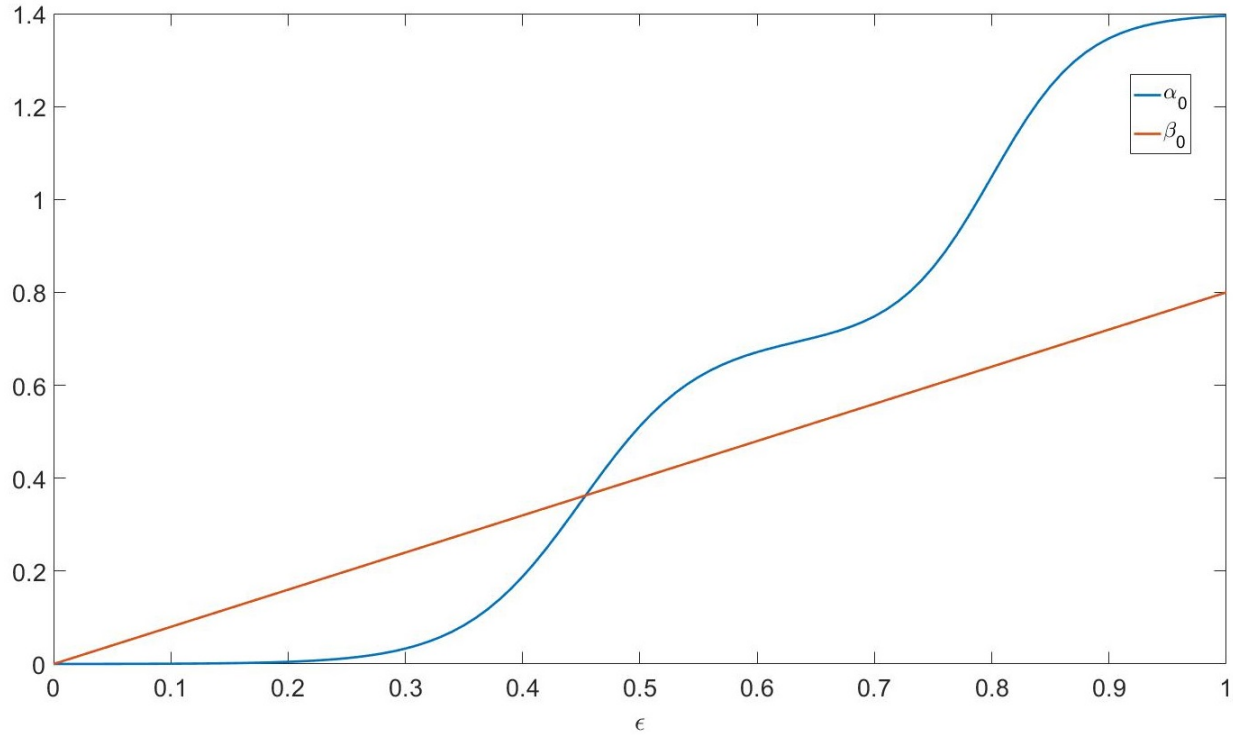

Figure S11: Trade-off functions for α_0 and β_0 that gives rise to evolutionary bistabilty demonstrated in Fig. S12.

Starting from several different possible initial conditions we found that the evolutionary parameters α and ϵ will evolve towards two distinct ESS pairs. This can be seen in Fig. S12(B) which demonstrates how the final ESS pairs can be dependent on the initial starting point of evolution. Therefore, if we start from different initial conditions we can have low or high evolutionary stable parasite virulence and hyperparasite strength.

Supplemental Material (not copyedited or formatted) for: Simran K. Sandhu, Andrew Yu. Morozov, Robert D. Holt, Michael Barfield. 2021. "Revisiting the Role of Hyperparasitism in the Evolution of Virulence." The American Naturalist 197(2). DOI: https://doi.org/10.1086/712351.

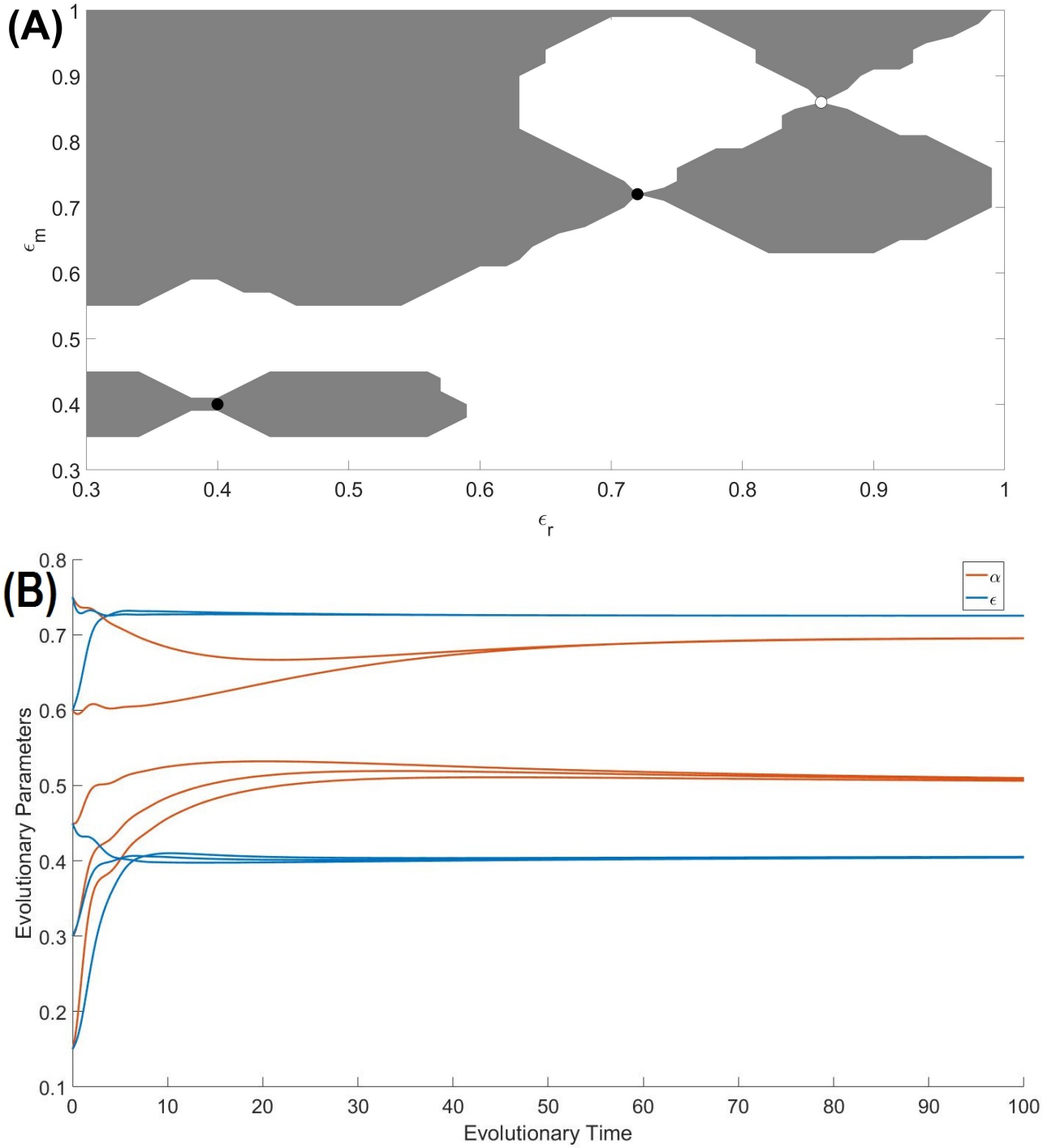

Figure S12: Evidence of bistability for the host-parasite-hyperparasite model allowing for the evolution of both the parasite and hyperparasite. (A) Firstly, we fix $\alpha = 0.6$ and construct a PIP that demonstrates the existence of two distinct evolutionary attractors given by the black filled points. (B) Secondly, we use the quantitative genetics with co-evolution to show the existence of two ESS pairs (α^*, ϵ^*) whose evolution is dependent on the initial evolutionary strategies. Initially, $\alpha = \epsilon = 0.15$, 0.3, 0.45 (which result in the lower ESS), or 0.6 or 0.75 (which result in the higher ESS). Other parameter values are as follows: $F(N) = 5 - 0.8N$, $\mu = 0.5$, $C = 1.5$, $K = 0.5$, $Q = 0.9$, $\sigma_0 = 0.5$.

Supplemental Material (not copyedited or formatted) for: Simran K. Sandhu, Andrew Yu. Morozov, Robert D. Holt, Michael Barfield. 2021. "Revisiting the Role of Hyperparasitism in the Evolution of Virulence." The American Naturalist 197(2). DOI: https://doi.org/10.1086/712351.

SM5 Co-Evolutionary Extinction

Within Section 3.3 of the main manuscript, an example of co-evolutionary extinction for our host-parasite-hyperparasite system with co-evolution of both the parasite virulence α and the hyperparasite strength ϵ was shown. Here we provide the regions of existence of each model component for all possible evolutionary parameter pairs. Demonstrating the extinction boundaries for each model component, shown in Fig. S13. The figure shows four regions; the dark blue region I represents where we have only uninfected susceptibles, the green region II we have susceptible hosts and hosts infected with the parasite only, the yellow region IV we have susceptible hosts and hosts infected with the hyperparasite only and finally the light blue region III we have the coexistence of all model components.

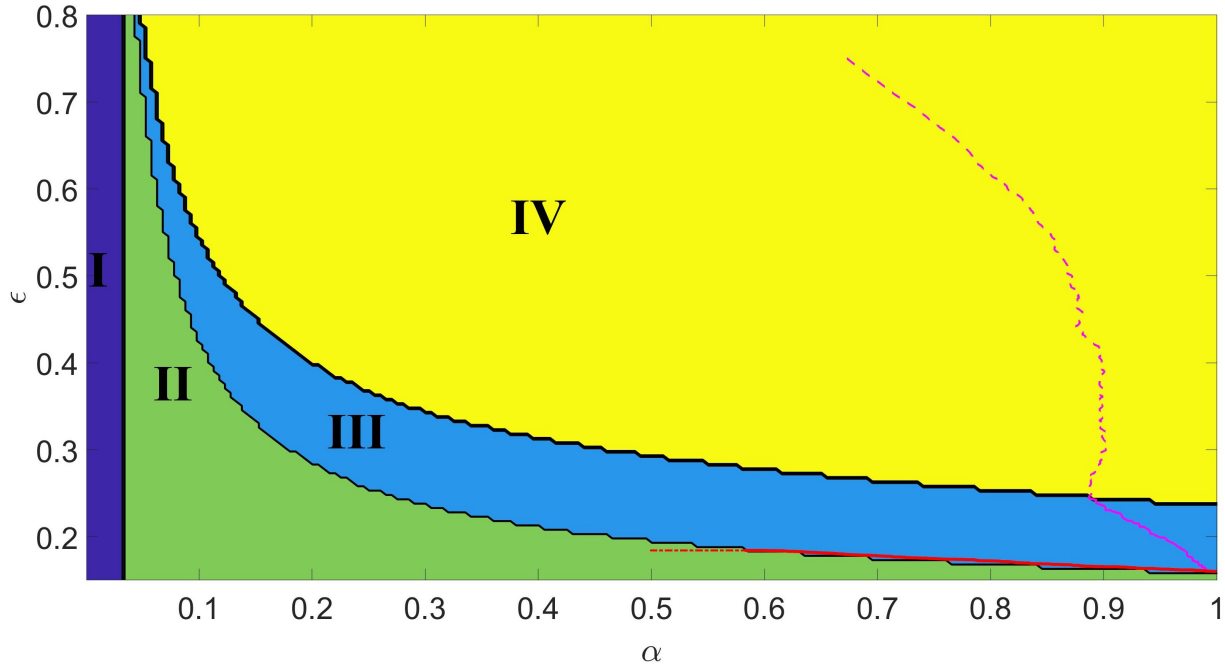

Figure S13: Regions of different model structures at the stationary states for different evolutionary parameter pairs (α, ϵ) corresponding to the example of co-evolutionary extinction shown in Fig.5 of the main text. Regions of the graph are as follows.(I)=The system consists of only susceptible hosts. (II)=The hyperparasite cannot be established in the system with the resulting system consisting of just susceptible hosts and hosts infected by the parasite. (III)=Coexistence of uninfected hosts and infected hosts with and without the hyperparasite. (IV)=At the equilibrium all pathogens are infected by the hyperparasite. The red and pink lines are two examples of phase plots of the evolutionary parameters α and ϵ (solid) and their subsequent evolution (dashed). The red curve is an example of the extinction of the parasite and the pink curve is an example of the extinction of the hyperparasite.

Fig. 5 in the main text demonstrates how the speed of evolution can impact the evolutionary outcome. For the quantitative genetics framework, we regulate speed by varying the values of G_α and G_ϵ (for fast evolution we have $G_\alpha = 0.05$, $G_\epsilon = 0.05$ and for slow evolution we have $G_\alpha = 0.05$, $G_\epsilon = 0.01$). However, for the adaptive dynamics framework, we instead regulate the speed through our choices of mutants. For a fast evolution, we allow the mutant to differ much more from the mutant than in the case with slower evolution. For each mutant, we select a random value with a uniform distribution over a range centred around the resident; the width of these ranges dictate the evolutionary speed. Interestingly, varying only the speed of evolution of ϵ results in different evolutionary outcomes, suggesting that if the hyperparasite evolves more slowly, it is subsequently eliminated by the parasite but if it evolves fast enough it will be able to invade all parasites.

Supplemental Material (not copyedited or formatted) for: Simran K. Sandhu, Andrew Yu. Morozov, Robert D. Holt, Michael Barfield. 2021. "Revisiting the Role of Hyperparasitism in the Evolution of Virulence." The American Naturalist 197(2). DOI: https://doi.org/10.1086/712351.

SM6 Comparison Between the Adaptive Dynamics and Quantitative Genetics Frameworks

Within Section 2 of the main manuscript, it was suggested that two approaches of modelling evolution can be applied to our host-parasite-hyperparasite model. The first one was the adaptive dynamics framework for which we construct the resident-mutant models (as displayed in the form of a flowchart in Section SM1). The second approach was based upon a quantitative genetics framework where we modelled the evolution from the equations (4)-(8) in the main text. Here we compare the two frameworks via direct simulations for all three evolutionary scenarios. Furthermore, we verify the obtained ESS through the use of eigenvalues; if we obtain a true evolutionary attractor then the eigenvalue should be negative in the vicinity of this point and zero at the point itself.

In Section 3.1 of the main text, we look at evolution in the parasite only. For this scenario we have the mutant equations given by equations (9) and (10) (displayed in Fig. S2 as a flowchart) from which the invasion fitness λ_P given by equation (11) can be derived. The resident-mutant model can be used to determine the ESS through a series of mutant invasions, where we simulate the behaviour of both the mutant and resident (using the model given by equations (1)-(3) in the main text) to determine which can survive, out-competing the other (to simulate their behaviour we implemented the ode45 MATLAB function). To determine the mutant strain we select a uniform random value close to that of the resident evolutionary parameter value. This is done by defining a range around the resident strain that the mutant must lie in; by varying the width of this range we can regulate the speed of the evolution (see section 3.3 and SM5). However, if this range is relatively large (sometimes required for computational speed) it can produce some computational errors resulting in slight oscillations around the true ESS (this can be seen in Fig. S14). Alternatively, we applied the quantitative genetics framework with $r_P = \max \lambda_P, \lambda_H$ in equation (7). The implementation of both frameworks is shown in Fig. S14(A), where it is clear that they both yield the same ESS parasite virulence α^*. Additionally, in Fig. S14(B) we can conclude that this ESS is indeed an evolutionary attractor.

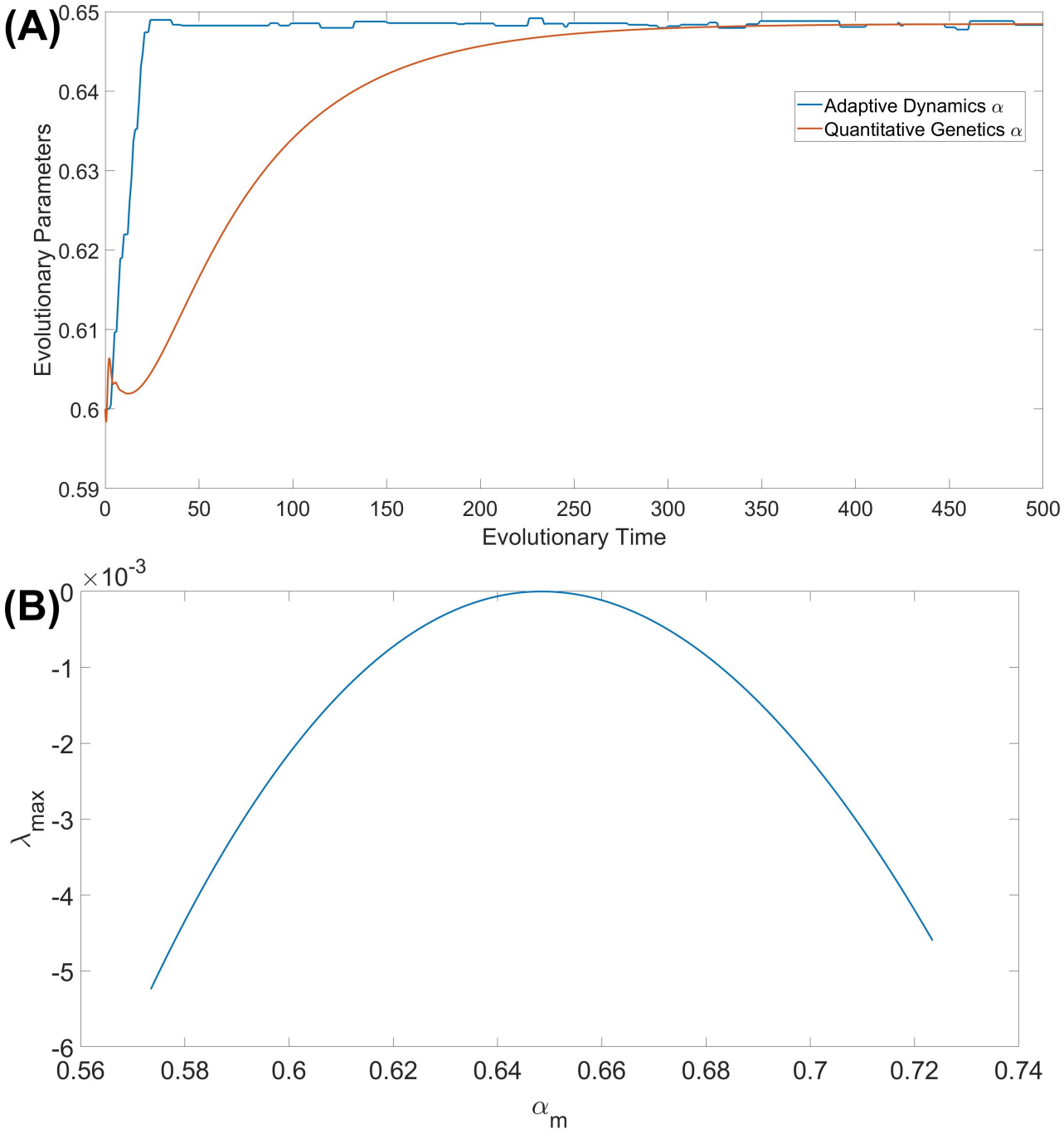

Figure S14: (A) Direct comparison of the adaptive dynamics framework and the quantitative genetics methodology as applied in Section 3.1 of the main manuscript, where we allow for evolution in the parasite only. We show the results of modelling the evolution of the parasite virulence using both frameworks showing they both yield the same ESS. (B) We verify these results through the computation of the dominant eigenvalue in the vicinity of the ESS α^*. Other parameter values are as follows: $F(N) = 5 - 0.8N$, $\mu = 0.5$, $C = 1.5$, $K = 0.5$, $Q = 0.9$, $\alpha_0 = 0.6$, $\beta_0 = 0.5$, $\sigma_0 = 0.5$, $G_\alpha = 0.005$, $G_\epsilon = 0.005$.

Section 3.2 of the main text explored the evolution in the hyperparasite only. For this case the mutant equation is given in the main text by equation (12) (or as a flowchart given by Fig. S3) with corresponding invasion fitness λ_H. For the quantitative genetics framework, we set $r_H = \lambda_H$ in equation (8) of the main

text. We applied both of these frameworks to each of the trade-off scenarios and the results can be seen in Fig. S15(A). In all cases, the ESS hyperparasite strength obtained from either framework yield the same result. Fig. S15(B) verifies that this singular point is an evolutionary attractor.

Supplemental Material (not copyedited or formatted) for: Simran K. Sandhu, Andrew Yu. Morozov, Robert D. Holt, Michael Barfield. 2021. "Revisiting the Role of Hyperparasitism in the Evolution of Virulence." The American Naturalist 197(2). DOI: https://doi.org/10.1086/712351.

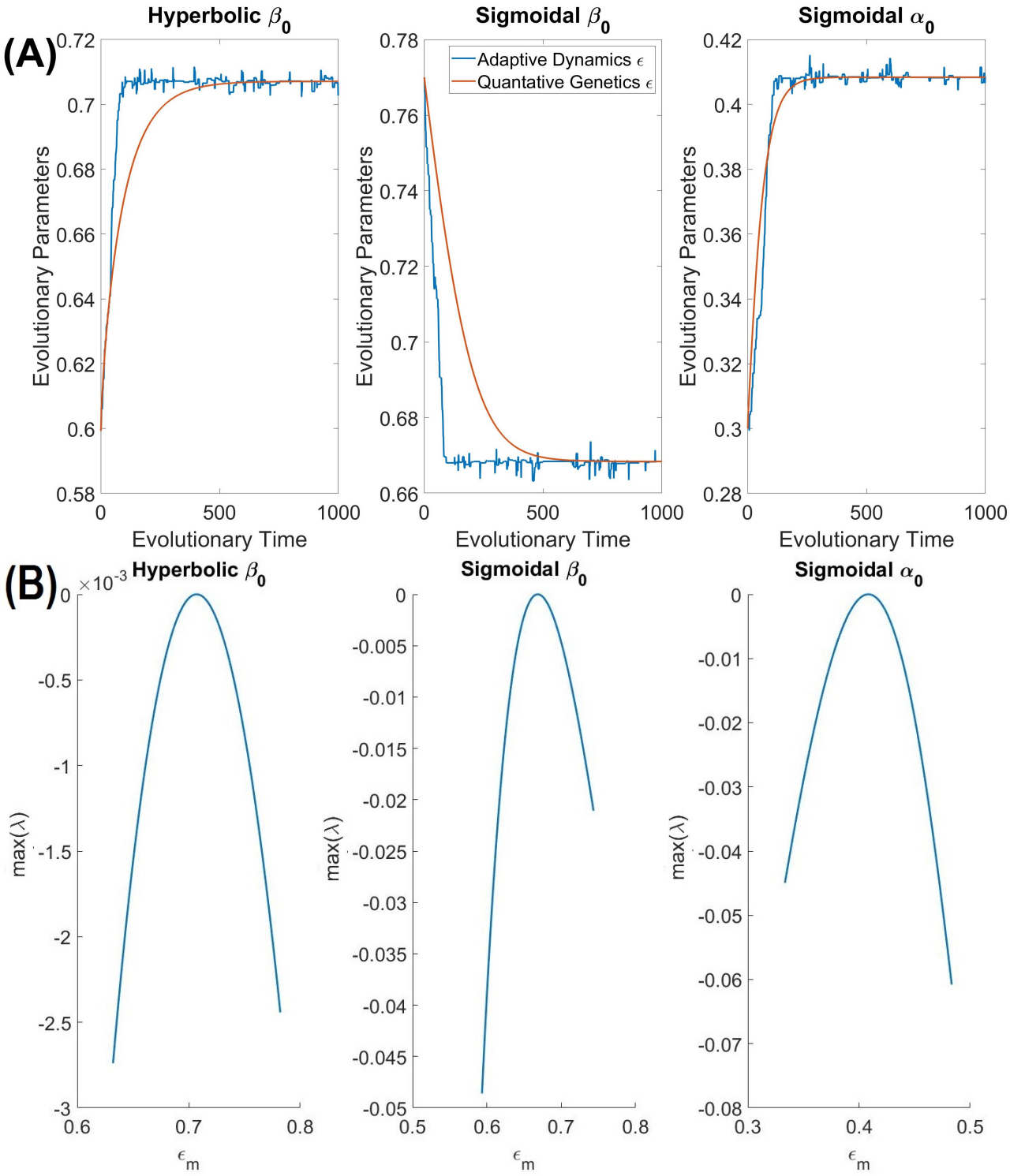

Figure S15: (A) Direct comparison of the adaptive dynamics framework and the quantitative genetics methodology outlined in Section 3.2 of the main manuscript where we allow for evolution in the hyperparasite only. We show the results of modelling the evolution of the hyperparasite strength using both frameworks showing they both yield the same ESS. (B) We verify these results through the computation of the dominant eigenvalue in the vicinity of the ESS ϵ^*. Other parameter values are as follows: $F(N) = 5 - 0.8N$, $\mu = 0.5$, $C = 1.5$, $K = 0.5$, $Q = 0.9$, $\sigma_0 = 0.5$, $\alpha = 0.6$, $G_\alpha = 0.005$, $G_\epsilon = 0.005$.

Supplemental Material (not copyedited or formatted) for: Simran K. Sandhu, Andrew Yu. Morozov, Robert D. Holt, Michael Barfield. 2021. "Revisiting the Role of Hyperparasitism in the Evolution of Virulence." The American Naturalist 197(2). DOI: https://doi.org/10.1086/712351.

Finally, Section 3.3 of the main text investigated the co-evolution of both the parasite and hyperparasite. For this scenario, the mutant equations are given in Appendix C of the main text (with the corresponding flowchart shown in Fig. S4). From these equations we obtained the invasion fitnesses λ_P, $\lambda_{H_{r,M}}$ (also given in Appendix C). Using $r_P = \lambda_P$ and $r_H = \lambda_{H_{r,M}}$ in equations (7) and (8) of the main text we can implement the quantitative genetics framework. Fig. S16(A) shows that in all trade-off scenarios considered, the ESS pairs (α^*, ϵ^*) are the same for both evolutionary frameworks. We again verify these ESS pairs through the use of the maximal eigenvalues and Fig. S16(B) demonstrates that they are indeed evolutionary attractors.

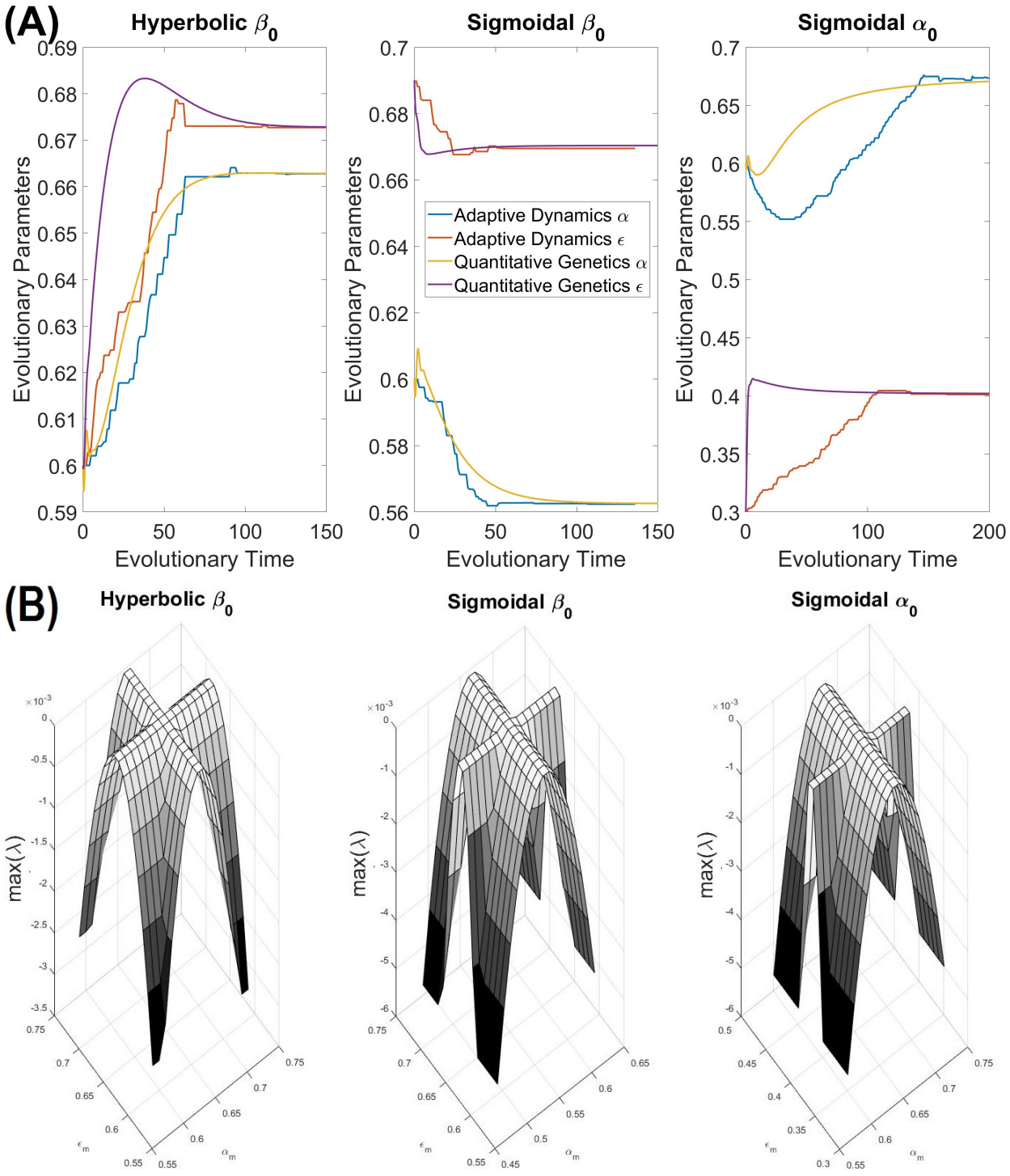

Figure S16: (A) Direct comparison of the adaptive dynamics framework and the quantitative genetics methodology outlined in Section 3.3 of the main manuscript where we allow for co-evolution in the both the parasite and hyperparasite. We show the results of modelling the evolution of the parasite virulence and hyperparasite strength using both frameworks showing they both yield the same ESS. (B) We verify these results through the computation of the dominant eigenvalue in the vicinity of the ESS α^* and ϵ^* Other parameter values are as follows: $F(N) = 5 - 0.8N$, $\mu = 0.5$, $C = 1.5$, $K = 0.5$, $Q = 0.9$, $\sigma_0 = 0.5$, $G_\alpha = 0.005$, $G_\epsilon = 0.005$.

Supplemental Material (not copyedited or formatted) for: Simran K. Sandhu, Andrew Yu. Morozov, Robert D. Holt, Michael Barfield. 2021. "Revisiting the Role of Hyperparasitism in the Evolution of Virulence." The American Naturalist 197(2). DOI: https://doi.org/10.1086/712351.

SM7 Mutual Displacement of Hyperparasite Strains

In section 3.4 of the main text, we introduce this idea of a hyperparasite strain displacing another in an infected host. Here, we show an example where we allow for evolution in the hyperparasite only with multiple stains of hyperparasite possessing the ability to displace neighbouring strains. The model equations can be modified to account for this and are given as follows;

$$\frac{dS}{dt} = F(N)S - \mu S - \left(\beta_P(\alpha)SP + \sum_{i=1}^{n} \beta_H(\alpha, \epsilon_i)SH_i\right) \tag{46}$$

$$\frac{dP}{dt} = \beta_P(\alpha)SP - \left(\sum_{i=1}^{n} \sigma(\alpha, \epsilon_i)PH_i\right) - \mu P - \alpha P \tag{47}$$

$$\begin{aligned}\frac{dH_i}{dt} = \beta_H(\alpha, \epsilon_i)SH_i + \sigma(\alpha, \epsilon_i)PH_i - \mu H_i - \alpha_H(\alpha, \epsilon_i)H_i - \gamma\sigma(\alpha, \epsilon_i)(H_{i-1} + H_{i+1})H_i + \\ \gamma\Big(\sigma(\alpha, \epsilon_{i+1})H_{i+1} + \sigma(\alpha, \epsilon_{i-1})H_{i-1}\Big)H_i\end{aligned} \tag{48}$$

where γ is the rate at which a hyperparasite of strain ϵ infects a host with a neighbouring hyperparasite strain with either ϵ_{i+1} or ϵ_{i-1} and displaces with resident hyperparasite. We simulated the behaviour of this model with a large range of ϵ values and we find that a large number of different strains are able to coexist in the system; the results can be seen in figure S17. The figure shows that multiple strains can coexist with their stationary density being larger the closer the strain is to ϵ^* verifying our earlier results. Fig. S17(A) shows only a limited number of ϵ values within the range 0 to 1, this shows how many strains will go extinct and only those close to the ESS (represented by the pink curve) can survive.

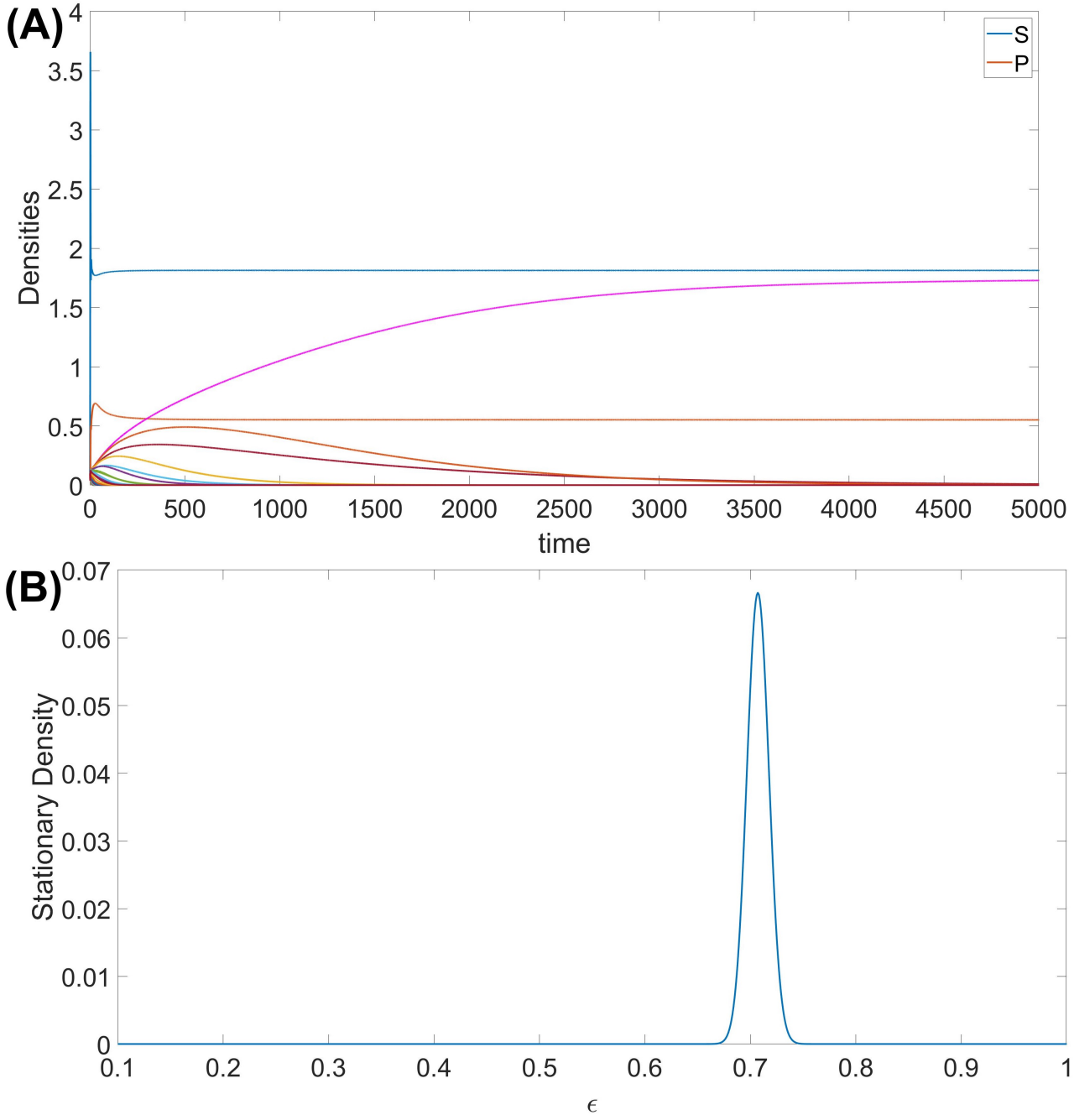

Figure S17: Addition of mutual displacement of hyperparasite strains into our model with evolution in the hyperparasite only with $\alpha = 0.6$ and trade-off functions given by $\alpha_0(\epsilon) = \epsilon$ with hyperbolic $\beta_0(\epsilon) = \frac{\epsilon}{0.6+\epsilon}$. We simulated the behaviour with multiple strains of hyperparasite present in the system. (A) Densities of susceptibles S, parasite-only hosts P, and hosts with a varying strains of hypereparasite H_i. (B) Distribution of the densities for each hyperparasite strain at the stationary state. Other parameter values are as follows: $F(N) = 5 - 0.8N$, $\mu = 0.5$, $C = 1.5$, $K = 0.5$, $Q = 0.9$, $\sigma_0 = 0.5$, $\gamma = 0.05$.

Note that, for clarity for the reader a larger grid is used to construct figure S17(A) than figure S17(B). Although the integral total density of hyperparasite remains the same for both figures due to the differences in grid size the maximal density will vary (in order to preserve this integral quantity).

Supplemental Material (not copyedited or formatted) for: Simran K. Sandhu, Andrew Yu. Morozov, Robert D. Holt, Michael Barfield. 2021. "Revisiting the Role of Hyperparasitism in the Evolution of Virulence." The American Naturalist 197(2). DOI: https://doi.org/10.1086/712351.

SM8 Proving Stability of Singularities

Within the appendixes of the main text we discuss the evolutionary stability of any singularity. We state that we have the following criteria that must be met to ensure stability;

$$E_i < 0, \quad E_i + M_i < 0, \quad \left| \frac{\partial^2 \lambda_P}{\partial \epsilon_R \partial \alpha_m} \frac{\partial^2 \lambda_{H_{rM}}}{\partial \alpha_R \partial \epsilon_m} \right| - (E_1 + M_1)(E_2 + M_2) < 0$$

where

$$E_1 = \frac{\partial^2 \lambda_P}{\partial \alpha_m^2} = \beta_P''(\alpha^*) S^* < 0, \quad M_1 = \frac{\partial^2 \lambda_P}{\partial \alpha_m \partial \alpha_r} = \beta_P'(\alpha) S'^*(\alpha),$$

$$E_2 = \frac{\partial^2 \lambda_{H_{rM}}}{\partial \epsilon_M^2} = \beta_0''(\epsilon^*)\beta_P(\alpha^*)(S^* + \sigma_0 P_r^*) - \alpha_0''(\epsilon^*)\alpha^*, \quad M_2 = \frac{\partial^2 \lambda_{H_{rM}}}{\partial \epsilon_M \partial \epsilon_R} = \beta_0'(\epsilon)\beta_P(\alpha)(S'^* + \sigma_0 P'^*),$$

In some of the cases with a trivial and semi-trivial state at the singularity these criteria can be proven analytically to always hold. However, for the more complex non-trivial state it is more difficult to verify. Therefore, we use computational results to show these criteria are met for varying parameter values. Firstly, we varied a single parameter and observed that the criteria is always met, we checked a wide range of parameters but here we just show the results when σ_0 is varied (shown in Fig. S18). Secondly, we conducted hundreds of random 'experiments' where parameter values are randomly selected and we find that all criteria are always satisfied.

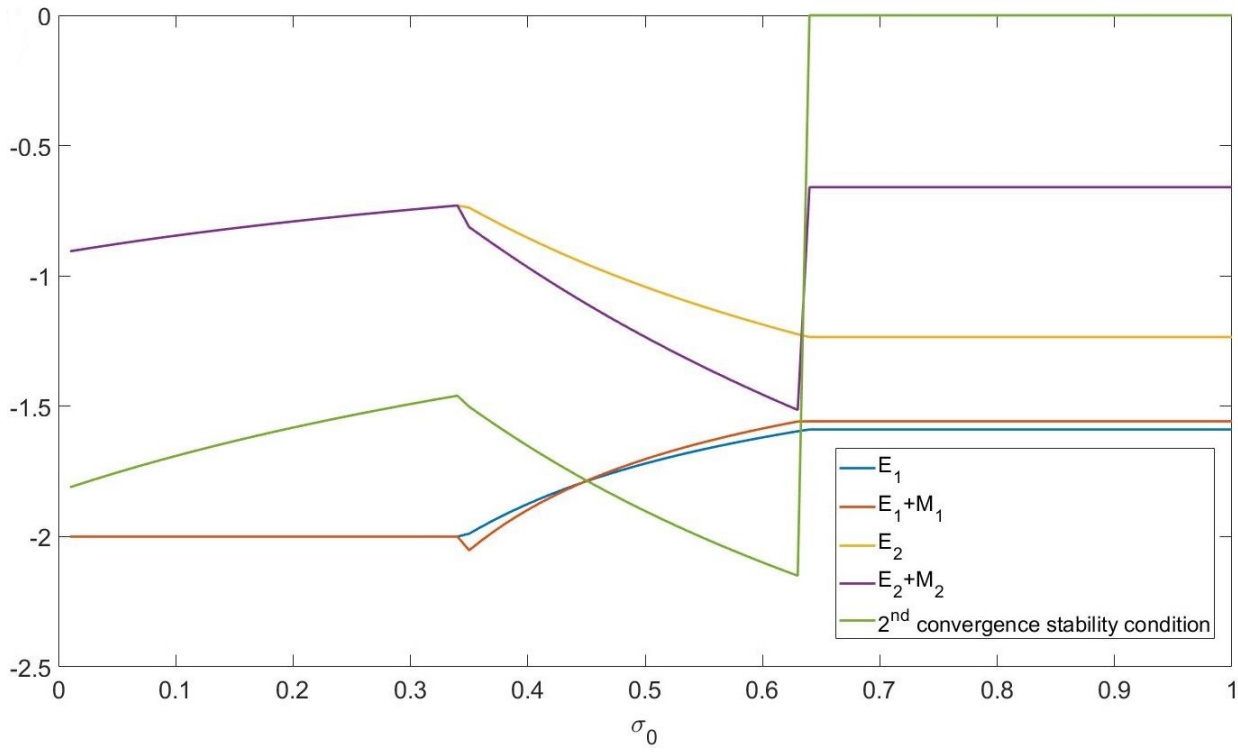

Figure S18: Computational verification of the criteria required for an evolutionary endpoint, or singularity to be stable. Dependence of the criterion on the parameter σ_0. Other parameter values are as follows: $F(N) = 5 - 0.8N$, $\mu = 0.5$, $C = 1.5$, $K = 0.5$, $Q = 0.9$ and trade-off functions given by $\alpha_0(\epsilon) = \epsilon$ with hyperbolic $\beta_0(\epsilon) = \frac{\epsilon}{0.6+\epsilon}$. The green line is close to 0 for high values of σ_0 but is always negative.

It is clear from the figures that the criteria is always met and the singularities are always either an evolutionary attractor or repellor.

Supplemental Material (not copyedited or formatted) for: Simran K. Sandhu, Andrew Yu. Morozov, Robert D. Holt, Michael Barfield. 2021. "Revisiting the Role of Hyperparasitism in the Evolution of Virulence." The American Naturalist 197(2). DOI: https://doi.org/10.1086/712351.

SM9 Hypervirulence

Within the main text, it is mentioned that we sometimes observe hypervirulence for our host-parasite-hyperparasite system, where $\alpha_0(\epsilon) > 1$. Here we provide an example that demonstrates the possibility of hypervirulence. In this case, we allowed for the co-evolution of both the hyperparasite and the parasite. Fig. S19 shows that the hyperparasite can evolve from a very low hyperparasite effect, $\alpha_0(\epsilon)$, to one that is greater than 1 making the hyperparasite more detrimental to the host than the parasite itself.

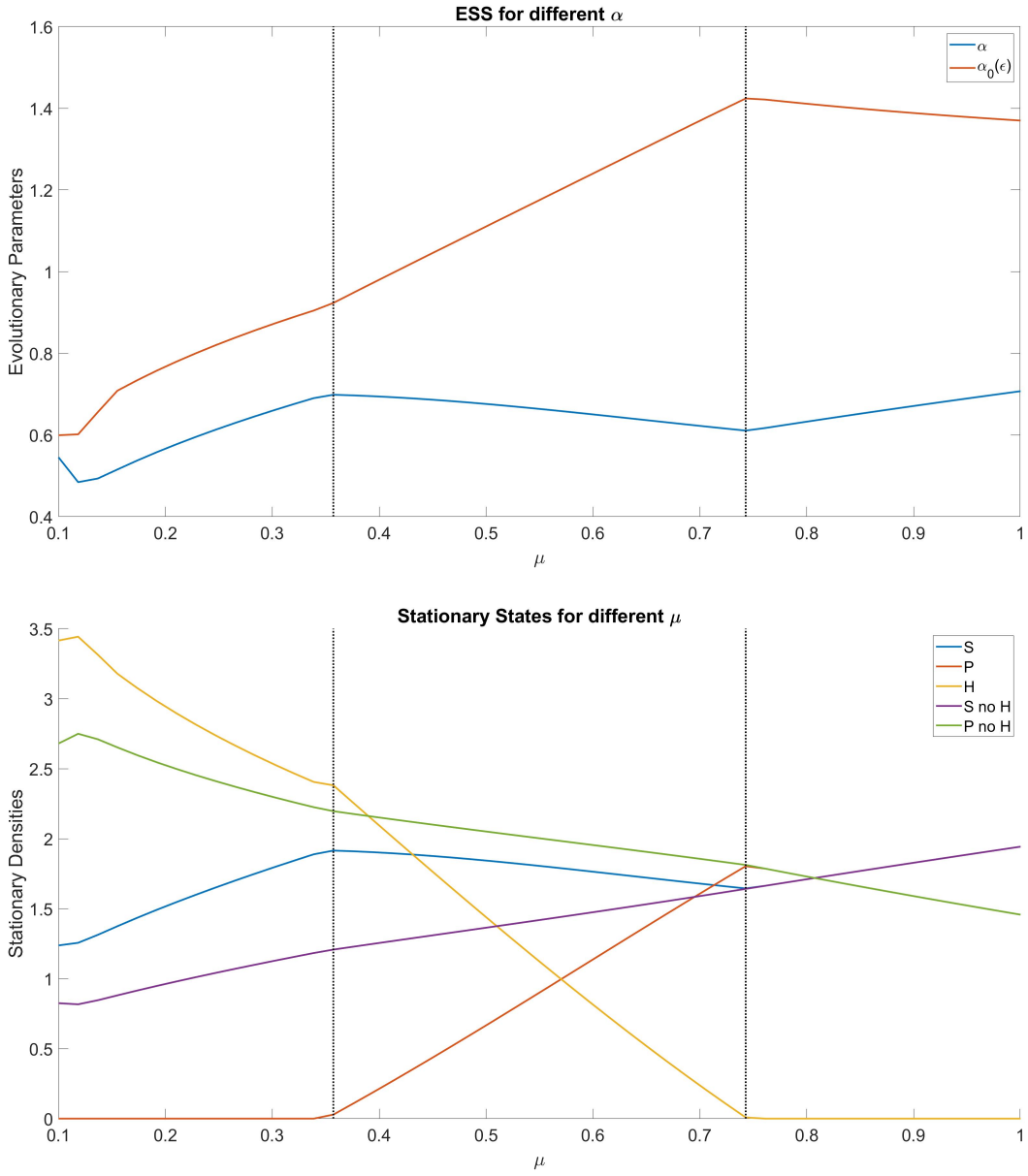

Figure S19: The dependence of model dynamics on the mortality rate μ where we allow for co-evolution in both the parasite and the hyperparasite with the trade-off functions given by $\alpha_0(\epsilon) = \epsilon$ with hyperbolic $\beta_0(\epsilon) = \frac{\epsilon}{0.6+\epsilon}$. (A) The ESS for the case with hyperparasite and without hyperparasite. (B) The equilibrium host densities at the ESS shown in (A). Regions (I)-(III) are defined the same as in Fig. 1 of the main manuscript. Other parameter values are as follows: $F(N) = 5 - 0.8N$, $C = 1.5$, $K = 0.5$, $\beta_0 = 0.5$, $Q = 0.9$, $\sigma_0 = 0.5$.